Galactic supernova remnants: an updated catalogue and some statistics

D. A. Green[*]

Mullard Radio Astronomy Observatory, Cavendish Laboratory, Madingley Road, Cambridge CB3 0HE, United Kingdom

Abstract. A catalogue of 231 Galactic supernova remnants (SNRs) is presented, and the selection effects applicable to the identification of remnants at radio wavelengths are discussed. In addition to missing low surface brightness remnants, small angular size – i.e. young but distant – remnants are also missing from the current catalogue of Galactic SNRs. Several statistical properties of Galactic SNRs are discussed, including the surface-brightness/diameter ($\Sigma-D$) relation. It is concluded that the wide range of intrinsic properties of Galactic remnants with known distances, together with the observational selection effects, means that use of the $\Sigma-D$ relation to derive diameters and hence distances for individual SNRs, or for statistical studies, is highly uncertain. The observed distribution of bright SNRs, which are thought to be largely free from selection effects, is also used to derive a simple model for the distribution of SNRs with Galactocentric radius.

Keywords : supernova remnants – catalogues – radio continuum: ISM – Galaxy: structure – ISM: general

1. Introduction

Our Galaxy contains over two hundred known Supernova Remnants (SNRs), which are an important source of energy and heavy element release into the interstellar medium (ISM), and are also thought to be the sites of the acceleration of cosmic rays. Over the last twenty years I have produced several versions of a catalogue of Galactic SNRs, the most recent revised in 2004 January (see Appendix A). Since the first version of the catalogue was published in Green (1984),

---

[*]e-mail: `D.A.Green@mrao.cam.ac.uk`

the number of identified Galactic SNRs has increased considerably, from 145 to 231, and here I review some of the statistical properties of Galactic remnants based on the most recent version of the catalogue. In Section 2 the catalogue is described, while the selection effects applicable to the identification of Galactic SNRs are discussed in Section 3. Some simple statistical properties of the remnants are presented in Section 4, with more detailed discussions of distance-dependant statistical studies of Galactic SNRs (including a brief discussion of some aspects of extragalactic remnants) and the Galactic distribution of SNRs given in Sections 5 and 6 respectively. The summary parameters of the 231 remnants from the 2004 January version of the catalogue of Galactic SNRs are presented in Appendix A.

2. The catalogue

The catalogue of Galactic SNRs contains: (i) basic parameters (Galactic and equatorial coordinates, size, type, radio flux density, spectral index, and other names); (ii) short descriptions of the observed structure at radio, X-ray and optical wavelengths, as applicable; (iii) other notes on distance determinations, pulsars or point sources nearby; and (iv) references. Appendix A gives the basic parameters of all 231 remnants in the 2004 January version of the catalogue, and describes these parameters in more details. The detailed version of the catalogue is available on the World-Wide-Web from:

http://www.mrao.cam.ac.uk/surveys/snrs/

which includes the descriptions, additional notes and references. The detailed version is available as postscript or pdf for downloading and printing, or as HTML web pages for each individual remnant. The web pages include links to the 'NASA Astrophysics Data System' for each of the nearly one thousand references. Notes both on those objects no longer thought to be SNRs, and on many possible and probable remnants that have been reported, are also included in the detailed version of the catalogue. In addition to the observational selection effects that are discussed further in Section 3, it should be noted that the catalogue is far from homogeneous. Is is particularly difficult to be uniform in terms of which objects are considered as definite remnants, and are included in the catalogue, rather than listed as possible or probable remnants which require further observations to clarify their nature. Although many remnants, or possible remnants, were first identified from wide area surveys, many others have been observed with a far from uniform set of observational parameters, making uniform criteria for inclusion in the main catalogue difficult. Also, some of the parameters included in the catalogue are themselves of quite variable quality. For example, the radio flux density of each remnant at 1 GHz. This is generally of good quality, being obtained from several radio observations over a range of frequencies, both above and below 1 GHz. However, for a small number of remnants – often those which have been identified at other than radio wavelengths – no reliable radio flux density, or only a limit is available (which applies to 14 remnants in the current catalogue).
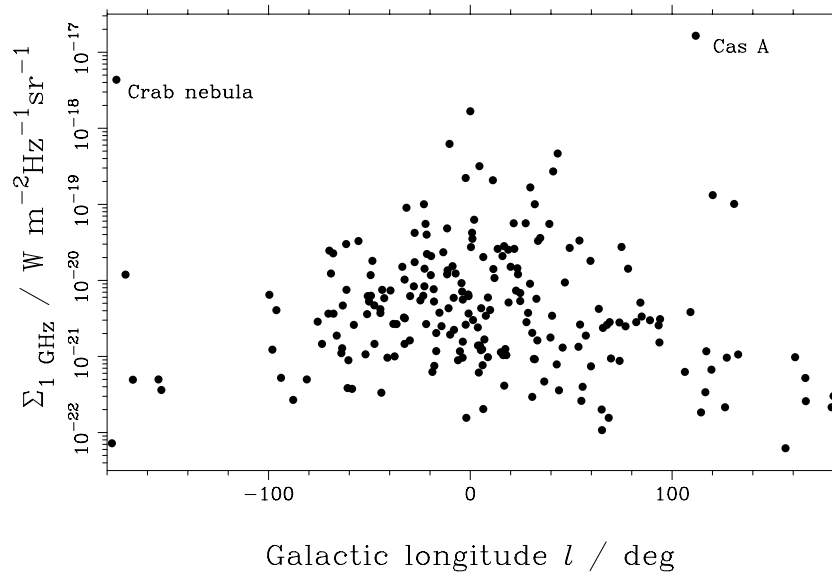
Figure 1. The distribution of surface brightness against Galactic longitude for all 217 Galactic SNRs with defined surface brightnesses.
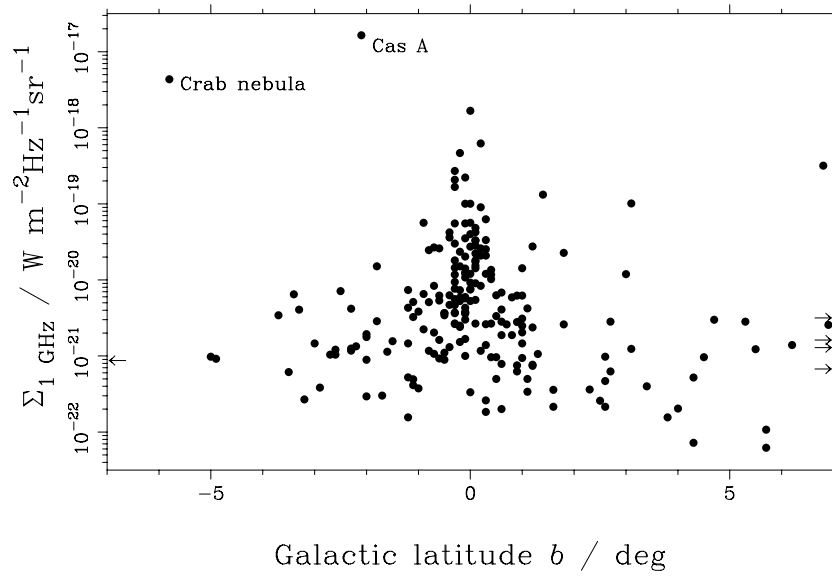

Figure 2. The distribution of surface brightness against Galactic latitude for 212 Galactic SNRs. The surface brightnesses of the five remnants with $|b| > 7°$ are indicated by arrows at the left and right edges of the plot.

3.   Selection effects

Although several Galactic SNRs have been identified at other than radio wavelengths, in practice the dominant selection effects are those that are applicable at radio wavelengths. Simplistically, two selection effects apply to the identification of Galactic SNRs (e.g. Green 1991), due to the difficulty in identifying (i) faint remnants and (ii) small angular size remnants. (In the case of extragalactic SNRs, the selection effects are different, and these are discussed briefly – particularly in the context of SNRs identified in M82 – in Section 5.3.)

3.1   Surface brightness

Clearly, SNRs need to have a high enough surface brightness for them to be distinguished from the background Galactic emission. This selection effect is *not* uniform across the sky, both because the Galactic background varies with position, and because the sensitivities of available wide area surveys covering different portions of the Galactic plane vary. The most recent large-scale radio surveys that have covered much of the Galactic plane are: (i) the Effelsberg survey at 2.7 GHz (Reich et al. 1990; Fürst et al. 1990), which covered $358° < l < 240°$ and $|b| < 5°$; and (ii) the MOST survey at 843 MHz (Whiteoak & Green 1996; Green et al. 1999), which covered $245° < l < 355°$, but only to $|b| < 1°.5$. Figs. 1 and 2 show the distribution of surface brightness for known SNRs against Galactic longitude and latitude. These show that in the anti-centre and away from $b = 0°$, where the Galactic background is lower, fainter remnants are relatively more common than brighter remnants, as expected. Also, there are fewer faint remnants identified in the 4th quadrant, which is due to the narrower range of the latitude coverage of the MOST survey compared with that of the Effelsberg survey. (There are similar numbers of remnants with surface brightnesses less than 10^{-21} W m^{-2} Hz^{-1} sr^{-1} with $|b| \lesssim 1°.5$, in the 1st and 4th quadrant – 9 and 7 respectively – but at higher Galactic latitude many more SNRs have been identified in the 1st quadrant than in the 4th – 10 compared to 5 – due to the wider latitude coverage of the Effelsberg survey.)

The Effelsberg survey detected new SNRs down to surface brightnesses corresponding to $\approx 2 \times 10^{-22}$ W m^{-2} Hz^{-1} sr^{-1} at 1 GHz (Reich et al. 1988), although the completeness limit for regions of brighter Galactic emission is higher. This is not only because of the difficulty in identifying remnants in the presence of extended Galactic emission, but is also due to confusion with bright H II regions (which is relatively more of a problem at higher frequencies). Since the new SNRs identified from the Effelsberg survey were included in the version of the SNR catalogue published in Green (1991), consideration of the surface brightness of other remnants in the survey region that have subsequently been identified is useful for estimating the completeness limit for this survey. Since 1991 an additional 24 remnants within $358° < l < 240°$ and $|b| < 5°$ have been included in the catalogue, most in the first quadrant. These remnants have been identified from a variety of observations, usually covering small regions of the Galactic plane, rather than from large area surveys. Of these, five do not have good radio observations available, and a histogram of the surface brightnesses of the remaining 19 is shown in Fig. 3. Of these
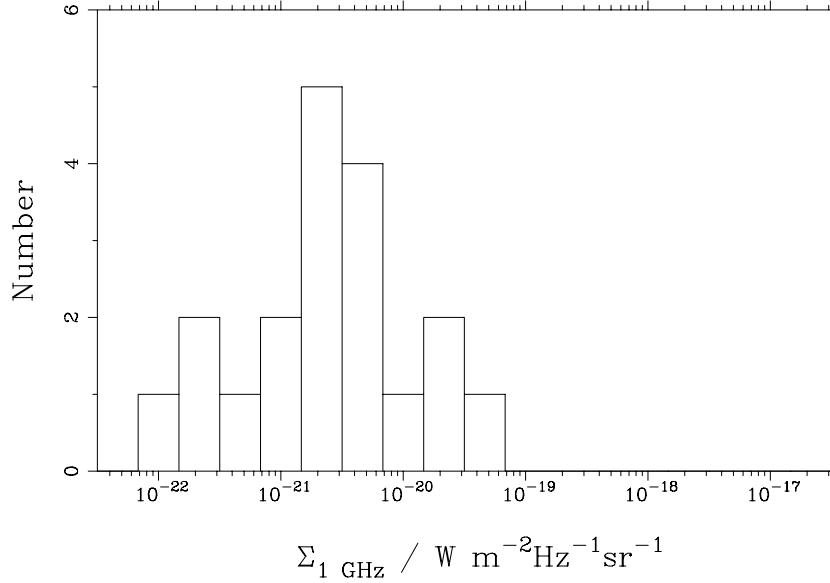
Figure 3. Histogram of the surface brightness of Galactic SNRs in the region $358° < l < 240°$, $|b| < 5°$ (i.e. the region covered by the Effelsberg 2.7-GHz survey, Reich et al. 1990; Fürst et al. 1990) identified since 1991 (cf. Fig. 4 for the distribution for all Galactic remnants).

remnants, three have surface brightnesses above 10^{-20} W m^{-2} Hz^{-1} sr^{-1}, two of which (G0·3+0·0 and G1·0−0·1) are close to the Galactic Centre, where the background is particularly bright. Regarding these three bright remnants as somewhat special cases, the surface brightnesses of the other more recently identified SNRs suggest a completeness limit of $\approx 10^{-20}$ W m^{-2} Hz^{-1} sr^{-1} for the Effelsberg survey.

It is difficult to estimate the completeness limit of the MOST survey in a similar way, as only three new remnants have been identified in the MOST survey region since the remnants identified in this survey were included in the 1996 version of the catalogue. This is due to the limited number of telescopes able to observe this part of the Galactic plane. Of these more recently identified, only two have surface brightnesses (of $\approx 5 \times 10^{-22}$ and 4×10^{-21} W m^{-2} Hz^{-1} sr^{-1} at 1 GHz). However, a comparison of the distribution of the brighter SNRs in Galactic longitude suggests that the completeness limit in the MOST survey region is not very different from that in the Effelsberg survey region. There are 32 remnants in the 1st quadrant (i.e. covered by the Effelsberg survey) with surface brightnesses above 10^{-20} W m^{-2} Hz^{-1} sr^{-1} and 27 in the 4th quadrant (i.e. covered by the MOST survey). Although the Molonglo survey covers a smaller range in Galactic latitude than the Effelsberg survey, this difference is not important, as only one of the bright remnants in the 1st quadrant has $|b| > 1°5$,

So, the surface brightness limit for completeness of the current catalogue of Galactic SNRs is approximately 10^{-20} W m^{-2} Hz^{-1} sr^{-1}. Fig. 4 shows a histogram of the surface brightnesses of
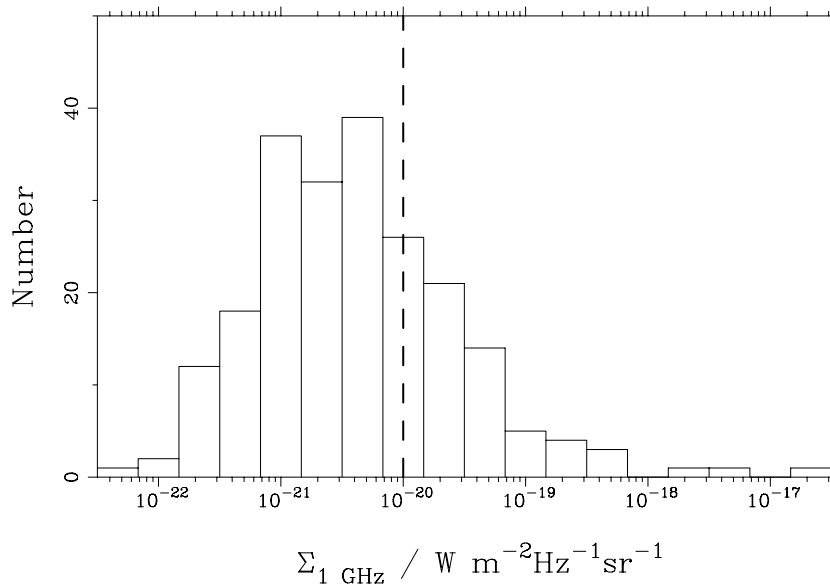
Figure 4. Distribution in surface brightness at 1 GHz of 217 Galactic SNRs. The dashed line indicates the surface brightness completeness limit discussed in Section 3.1.

the 217 Galactic SNRs, of which 64 are above this nominal surface brightness limit. As noted above, many SNRs with surface brightnesses below this limit have been identified, both from surveys and from other observations. These fainter remnants are predominantly in regions of the Galaxy where the background is low, i.e. in the 2nd and 3rd quadrants, and away from $b = 0\,°$, as shown in Fig. 5.

It is noticeable in Fig. 1 that there are more remnants in the 2nd quadrant than the 3rd (21 compared with 11). It seems likely that this is due to the fact that the 2nd quadrant is more accessible to the wider range of northern hemisphere radio telescopes than is the 3rd quadrant. Above the nominal surface brightness limit given above, there are only very few remnants in the 2nd and 3rd quadrants (3 and 2 respectively), i.e. for these bright remnants there is no indication of any obvious deficit of remnants in the 3rd quadrant. At first sight, Fig. 2 appears to show that there are more remnants identified away from the Galactic plane at positive latitudes than at negative latitudes. There is an asymmetry in the number of SNRs at high Galactic latitudes. There are 11 remnants with $|b| \geq +5°$, but only 4 remnants with $|b| \leq -5°$. Most of these high positive latitude remnants are in the 1st and 2nd quadrants, which suggests this asymmetry is related to Gould's Belt (e.g. Stothers & Frogel 1974), which is predominantly at positive latitudes in these quadrants. However, it is not clear that these high latitude remnants are close enough to be associated with Gould's Belt. There is no evidence for any asymmetry in the number of remnants at low Galactic latitudes; there are 49 with $b \geq +1°$ and 44 with $b \leq -1°$, which are not statistically different.

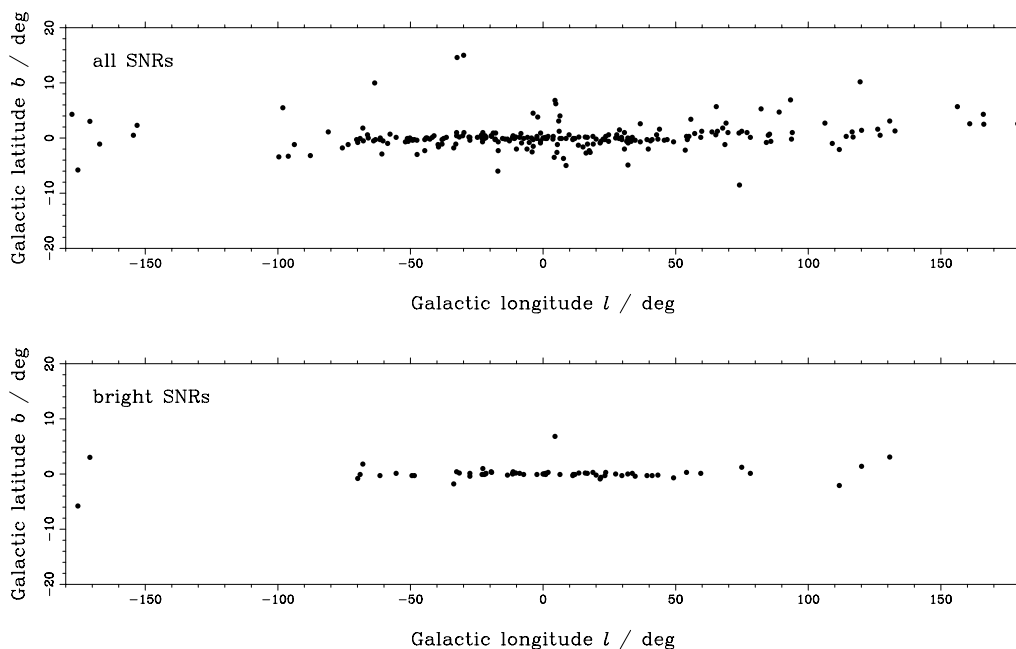Ongoing and future observations will no doubt continue to detect more Galactic SNRs, al-

Figure 5. Galactic distribution of (top) all Galactic SNR and (bottom) those SNRs with a surface brightness at 1 GHz greater than 10^{-20} W m^{-2} Hz^{-1} sr^{-1}. (Note that the latitude and longitude axes are not to scale.)

though it seems very likely that most of these objects will be faint, and hence difficult to study in detail. Currently there are several large scale radio surveys underway that will cover much of the Galactic plane including[1]: (i) the Canadian Galactic Plane Survey (CGPS, see: Taylor et al. 2003) which covers much of the northern Galactic plane, from $l \approx 55°$ to $l \approx 195°$; (ii) the VLA Galactic Plane Survey (VGPS, see: Lockman & Stil 2004) which covers $l = 18°$ to $l = 67°$, (iii) the Southern Galactic Plane Survey (SGPS, see McClure-Griffiths et al. 2001; McClure-Griffiths 2002), and (iv) the second-epoch Molonglo Galactic Plane Survey (MGPS2, see Green 2002), which covers $240° \leq l \leq 5°$, $|b| \leq 10°$. Examples of recently identified SNRs include two faint remnants with surface brightnesses at 1 GHz less than a few time 10^{-22} W m^{-2} Hz^{-1} sr^{-1}, which were found from CGPS observations by Kothes et al. (2001). However, confusion with the Galactic background – particularly in regions near the Galactic Centre and near $b = 0°$ – will continue to be a limiting factor in the identification of even moderately bright remnants. Comparison of radio observations over a wide range of frequencies (so spectral index information can be used), or observations at other than radio frequencies, may help to avoid some of the limits caused by this confusion. Recent discoveries include three new[2], faint SNRs near $l = 11°$ from Brogan et al. (2004), which have surface brightness at 1 GHz of $(2–6) \times 10^{-21}$ W m^{-2} Hz^{-1} sr^{-1}. These

---

[1] Also see: `http://www.ras.ucalgary.ca/IGPS/` for further information on the first three of these surveys.

[2] These remnants are not included in the catalogue presented in Appendix A, as their identification was published after that catalogue was updated in 2004 January.
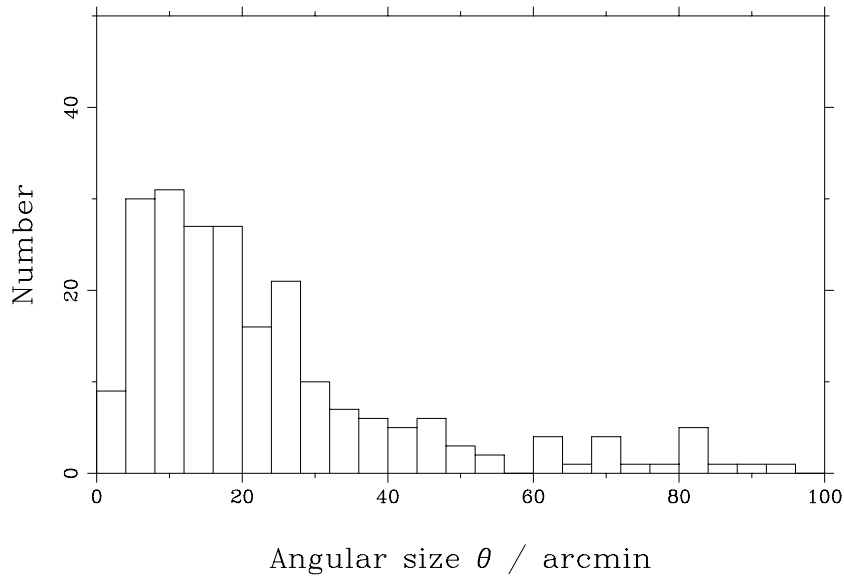
Figure 6. Histogram of the angular size of 219 Galactic SNRs (12 remnants larger than 100 arcmin are not included).

new remnants were identified because of the wide range of frequencies, and the relatively high resolution of the radio observations.

As discussed below in Section 5.2, there is a general trend that fainter remnants tend to be larger, and hence on average older, than brighter remnants. However, because of the wide range of properties of Galactic SNRs with known distances, the surface brightness selection effect applies not just to old remnants, but also to young remnants. In particular, note that the remnant of the SNR of AD 1006 (see Table 1, below) is fainter than the surface brightness completeness limit discussed above.

It should be noted that the study of Galactic SNRs by Filipović et al. (2002), which used the PMN Southern Survey images to extract flux densities of SNRs at 5 GHz, is seriously limited by observational constraints. Since the PMN observations were not processed to image extended objects (see Condon, Griffith & Wright 1993), the derived flux densities of many SNRs are in serious error.

3.2   Angular size

Small angular size SNRs are likely to be missing from current catalogues. If they are too small, then their structure is not well resolved by the available Galactic plane surveys, and they would not be recognised as likely SNRs. Fig. 6 shows the histogram of the angular sizes of known

remnants, which peaks at around 10 arcmin. (Note that for elongated remnants, which have angular sizes given as $n \times m$ arcmin^2 in the catalogue, a single diameter of $\sqrt{nm}$ has been used in this histogram, and in other figures in this paper concerned with angular size.) The limiting angular size varies for the different available wide area surveys. As discussed above, the radio survey that covers most of the Galactic plane is the Effelsberg 2.7-GHz survey, which has a resolution of ≈ 4.3 arcmin. So, for this survey, any remnants less than about 13 arcmin in diameter (i.e. 3 beamwidths) are not likely to be recognised from their structures (although, as discussed in Section 3.3, some searches have been made for small remnants among the unresolved and barely resolved sources in the Effelsberg 2.7-GHz survey). The MOST 843-MHz survey has a much better resolution, ≈ 0.7 arcmin, which implies that in the region of the Galactic plane covered by this survey only remnants smaller than about ≈ 2 arcmin (i.e. 3 beamwidths) might be expected to be missed. However, although the MOST survey detected 18 new SNRs (Whiteoak & Green 1996), the smallest new remnant is G345·7−0·2, which is 7×5 arcmin^2 in extent, i.e. several times larger than the nominal limit of ≈ 2 arcmin. Thus it is difficult to quote a single angular size selection limit for current SNR catalogues, although it is clear that it is difficult to identify small angular size remnants from existing wide area surveys.

This selection effect is likely to be more important for filled-centre type remnants than for shell type remnants. Even if filled-centre remnants are large enough to be resolved in a survey at the level of several beamwidths, their centrally brightened structures may not be striking enough to be able to recognise them as filled-centre remnants. Using only radio continuum observations, it is also easy to confuse the flat-spectrum synchrotron emission from filled-centre remnants with thermal emission. Additional observations – e.g. radio polarisation (as used to identify the small angular size filled-centre remnant G54·1−0·3, see Reich et al. 1985), radio recombination line non-detections (see, for example, Misanovic, Cram & Green 2002), relatively low infra-red to radio ratios (e.g. Cohen & Green 2001), X-ray emission (e.g. Schaudel et al. 2002) – are useful to distinguish filled-centre remnants from thermal sources.

3.3 Missing young but distant SNRs

The lack of small angular size remnants – i.e. young but distant remnants – is particularly clear when the remnants of known 'historical' Galactic supernovae (see Stephenson & Green 2002) are considered. These remnants are relatively close-by – as is expected, since their parent SNe were seen historically – and therefore sample only a small fraction of the Galactic disc. Consequently we expect many more similar, but more distant remnants in our Galaxy (e.g. Green 1985), but these are not present in current catalogues.

Table 1 gives the distances, angular sizes, flux densities and surface brightnesses at 1 GHz, for the remnants of known historical supernovae from the last thousand years, plus Cas A (which although its progenitor was not seen – so it is not strictly a historical remnant – is known to be only about 300 years old). The distances used for these remnants are those given in Section 5.1. This table also lists the parameters of these remnants when scaled to larger distances of 8.5 and 17 kpc, i.e. to represent how they would appear if they if they were at the other side of the Galaxy

Table 1. Parameters of known historical SNRs, plus Cas A.

date	name or remnant	distance /kpc	size /arcmin	$\Sigma_{1\,\mathrm{GHz}}$ /W m^{-2} Hz^{-1} sr^{-1}	$S_{1\,\mathrm{GHz}}$ /Jy	size /arcmin	$S_{1\,\mathrm{GHz}}$ /Jy	size /arcmin	$S_{1\,\mathrm{GHz}}$ /Jy
				as observed		if at 8.5 kpc		if at 17 kpc	
–	Cas A	3.4	5	1.6×10^{-17}	2720	2.0	435	1.0	109
AD 1604	Kepler's	2.9	3	3.2×10^{-19}	19	1.0	2.2	0.5	0.55
AD 1572	Tycho's	2.3	8	1.3×10^{-19}	56	2.3	4.1	1.1	1.0
AD 1181	3C58	3.2	7	1.0×10^{-19}	33	2.6	4.7	1.3	1.2
AD 1054	Crab nebula	1.9	6	4.4×10^{-18}	1040	1.4	52	0.7	13
AD 1006	G327·6+14·6	2.2	30	3.2×10^{-21}	19	7.7	1.3	3.9	0.31

(from the Galactic Centre, to the far point on the Solar Circle). The number of other young (i.e. less than a thousand year old) SNRs expected in the Galaxy can be estimated in two simple ways: (i) from the expected supernova rate of one every 45 to 70 years (Cappellaro 2003), 15 to 22 young remnants are expected in total; (ii) considering the fraction of the Galactic disc sampled by the historical supernovae (6 in a thousand years), which are within $\approx$ 4 kpc, i.e. about 16 per cent of the Galactic disc modelled as being uniform and having a radius of $\approx$ 10 kpc, implies there should be $\approx$ 40 young remnants (see also the discussions in Strom 1994). Of these, $\approx$ 80% (see Cappellaro 2003) are expected to be the remnants of massive supernovae – i.e. from type Ib/Ic/II SNe – and therefore be close to the Galactic plane.

From Table 1, any young SNRs in the Galaxy similar to the known historical remnants, but in the far half of the Galaxy, would generally be expected to have angular sizes less than a few arcmin, high surface brightness, greater than $\approx 10^{-19}$ W m^{-2} Hz^{-1} sr^{-1} (although remnants similar to the remnant of the SN of AD 1006 would be much fainter). These remnants would also be expected to lie close to the Galactic plane, with $|b| \lesssim 1°$. Although the above estimates are rather uncertain due to intrinsic Poisson uncertainties from the small numbers of known historical remnants, they imply that about a dozen or more young but distant remnants might be expected. However, there are very few such remnants in the current Galactic SNR catalogue. In fact there are only 3 known remnants with angular sizes of 2 arcmin or less: G1·9+0·3, G54·1+0·3 and G337·0−0·1. Of these, G1·9+0·3 is the smallest, with an angular size of only 1.2 arcmin. No distance measurement is available for this remnant – which being close to $l = 0°$ makes kinematic methods unreliable – but even if it were at the far side of the Galaxy, at say 17 kpc, its physical size would only be 6 pc. This is comparable to the sizes of the known historical remnants in Table 1 (which have physical diameters of 5, 3, 5, 7, 3 and 19 pc respectively). Another indication that this is indeed a young remnant is that it shows a circularly symmetric limb-brightened shell of radio emission (see Fig. 7 for a previously unpublished image of this remnant at 1.5 GHz, from 1985 observations made with the NRAO's VLA[3]). The known young shell remnants all show highly circular structures, whereas older remnants tend to be less circular, as is expected as they expand into differing regions of the interstellar medium. The distance to the filled-centre remnant

---

[3]The National Radio Astronomy Observatory is a facility of the National Science Foundation operated under cooperative agreement by Associated Universities, Inc.
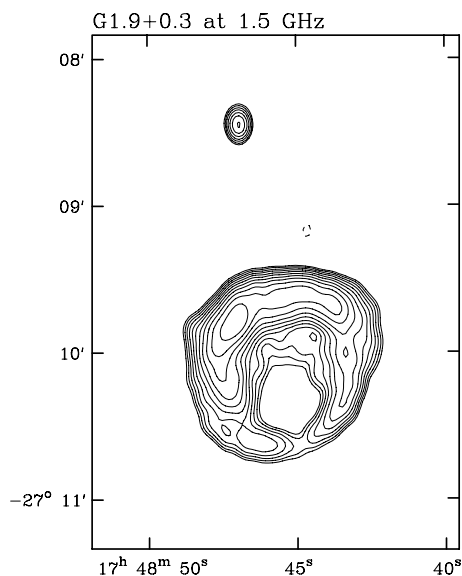
Figure 7. A VLA image of G1·9+0·3 at 1.5 GHz, with a resolution of 9.4 × 7.2 arcsec^2 at a position angle of 3°. The contour levels are at −1, 1 $\sqrt{2^n}$ mJy beam^{-1} for $n = 0, 1, 2 \ldots$ (with the negative contour dashed). The coordinates are J2000.0.

G54·1+0·3 is uncertain (e.g. Camilo et al. 2002), although its small angular size of 1.5 arcmin again suggests it is physically small, and therefore young, even if it were to be situated at the edge of the Galaxy. A reasonably accurate distance estimate is available for G337·0−0·1 (see Section 5.1), and this is ≈ 11 kpc, which is consistent with this being a young but distant SNR (with a diameter of ≈ 5 pc, from its angular size of 1.5 arcmin). The deficit of small remnants is also illustrated in Fig. 8, which shows there are very few known Galactic remnants with high surface brightnesses and small angular sizes.

This deficit of young but distant remnants has long been recognised, but searches for remnants of this type (e.g. Green & Gull 1984; Helfand et al. 1984; Green 1985, 1989; Sramek et al. 1992; Misanovic et al. 2002; see also Saikia et al. 2004) have had only limited success (identifying the small remnants G1·9+0·3 and G54·1+0·3 noted above). Since the missing young but distant remnants are expected to have angular sizes of a few arcmin or less, they will not have been resolved sufficiently by single-dish radio surveys with resolutions of several arcminutes, so will not have been recognised as SNRs. Searching for these remnants is not easy because there are very many candidate sources in single-dish surveys to choose from (e.g. in the 1st quadrant, there are over a thousand compact sources in the Effelsberg survey with $|b| \leq 1°$), and only a fraction of these have been observed with high enough resolution to be able to identify them if they were small angular size SNRs. Moreover, the missing young but distant remnants are likely to be in the most complex, and hence most confused, regions of the Galactic plane, as being distant they will be close to $b = 0°$. The use of additional observational indicators (e.g. radio spectral index, infra-red to radio ratios) has yet not proved efficient for improving such searches, nor have

D. A. Green
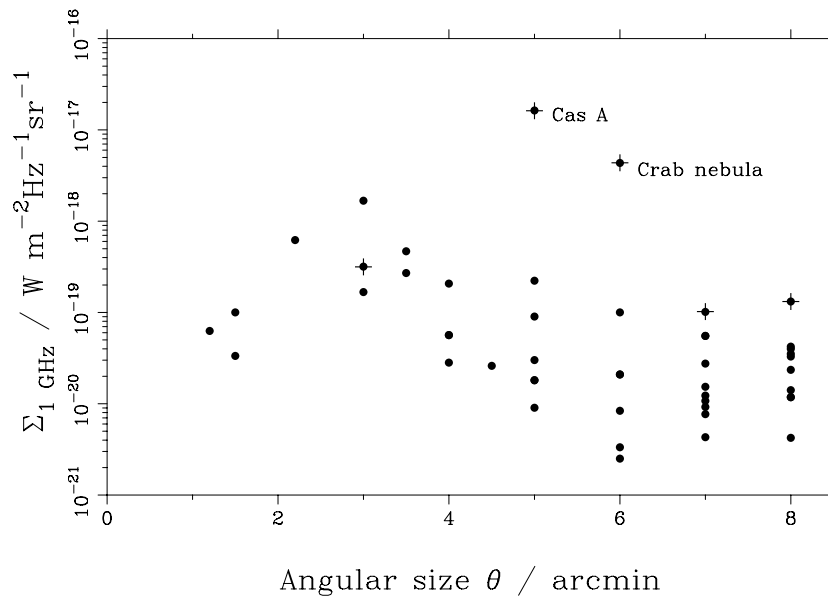
Figure 8. Distribution in surface brightness at 1 GHz against angular size for known Galactic SNRs of angular size ≤ 8 arcmin. The five historical remnants from Table 1 included in this plot are indicated by additional crosses. (For all but the smallest few remnants in the catalogue, the angular size is given to the nearest arcmin.)

the MOST survey (see Whiteoak & Green 1996) and the NVSS (see Condon et al. 1998), which cover the Galactic plane with slightly higher resolution than available single-dish surveys. (Note, however, that the NVSS does contain previously unrecognised SNRs, for example G353·9−2·0, with an angular size of 13 arcmin, see Green 2001a.) The fact that such missing, small remnants are likely to be in complex regions of the plane may mean that confusion is a very significant problem, and not just at radio wavelengths. Further searches for these missing young but distant remnants are required.

It should be noted that there are unlikely to be other luminous remnants in the Galaxy like Cas A and the Crab nebula. Any such remnants, even on the far side of the Galaxy, would have relatively high flux densities, and the nature of all such sources in the Galactic plane is known. On the other hand, the remnant of the SN of AD 1006 is faint – possibly because it is far from the Galactic plane, in a low density region – and distant remnants similar to this would be particularly difficult to detect, as they would have both a small angular size and low surface brightness. However, any remnants similar to the other three historical remnants are detectable.
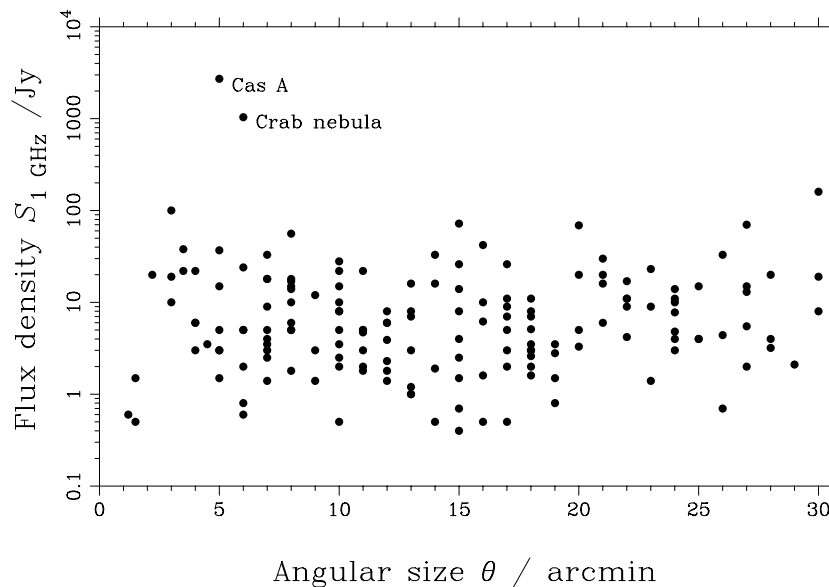
Figure 9. Distribution of flux density at 1 GHz against angular size for known Galactic SNRs with diameters ≤ 30 arcmin.

4. Some simple SNR statistics

In the current version of the catalogue, 77% of remnants are classed as shell (or possible shell), 12% are composite (or possible composite), and 4% are filled-centre (or possible filled centre) remnants. The remaining 7% have not yet been observed well enough to be sure of their type, or else are objects which are conventionally regarded as SNRs although they do not fit well into any of the conventional types (e.g. CTB80 (=G69·0+2·7), MSH 17−39 (=G357·7−0·1)). Since the 1991 version of the catalogue (Green 1991), the proportion of shell remnants in the catalogue has stayed very similar, with the proportion of composite remnants increasing from 8%, and the proportion of filled centre remnants has decreased from 7%. The increase in the proportion of composite remnants is because more recent, improved observations have continued to identify many more shell remnants, but have also identified faint, pulsar powered nebulae in what until then had been identified as pure shell remnants (e.g. W44 (=G24·7−0·4)), and also that faint shells have been detected around some filled-centre remnants (e.g. G21·5−0·9).

There are 14 Galactic SNRs that are either not detected at radio wavelengths, or are poorly defined by current radio observations, so that their flux density at 1 GHz cannot be determined with any confidence: i.e. 94% have a flux density at 1 GHz included in the catalogue. Of the catalogued remnants, 36% are detected in X-ray, and 23% in the optical. At both these wavelengths, Galactic absorption hampers the detection of distant remnants.

Some of the properties of the Galactic SNRs in the catalogue, which are not shown in other

sections of this paper, are shown in Fig. 9. This shows the flux density at 1 GHz versus angular size for SNRs less than 30 arcmin in extent. This is of interest in terms of which remnants may appear as bright, relatively compact Galactic plane sources (e.g. in future Planck surveys). The most prominent sources are, not surprisingly, the very bright SNRs Cas A and the Crab nebula (see Table 1), which have similar angular sizes, and very high flux densities. Cas A has the higher flux density at 1 GHz by a factor of about 2.6, but because the Crab nebula has a much flatter spectrum (with $\alpha \approx 0.30$ compared with ≈ 0.77 for Cas A, e.g. Baars et al. 1977), the Crab nebula has the higher flux density at frequencies above about 8 GHz. The statistics of the radio spectral indices of Galactic SNRs are not discussed here, although there is a short discussion of these in Green (2001b).

5. Distance dependant SNR statistics

5.1 Distances to SNRs

Many studies of Galactic SNRs require knowledge of the distances to remnants (or equivalently their physical sizes, since their angular sizes are known). However, accurate distances are not available for many known SNRs. The distances that are available are obtained from a wide variety of methods – e.g. optical expansion and proper motion studies, 21-cm H I absorption spectra, H I column density (see Foster & Routledge 2003), association with H I or CO features in the surrounding interstellar medium, or association with other objects – each of which is subject to their own uncertainties, and some of which are subjective. Table 2 presents distances for 47 Galactic SNRs available in the literature. (In a few cases distance estimates to SNRs are also available from the distances to associated pulsar, derived from the observed pulsar dispersion measure and a model of the Galactic electron density distribution. However, these have not been used in Table 2.) In several cases the distances derived from H I absorption measurements have been recalculated using a modern 'flat' rotation curve with a Galactocentric radius of 8.5 kpc and a constant rotation speed of 220 km s^{-1}. Additionally, in a few cases the distances given depend on re-interpretation of the published observations. For G11·2−0·3 and G21·5−0·9, the distances given correspond to the near distances of the last strong H I absorption seen (see also Safi-Harb et al. 2001 for G21·5−0·9).

The uncertainties in these distances are far from uniform. For kinematic distances – which are a large majority of the distances given in Table 2 – there are always some uncertainties in deriving distances from observed velocities, due to deviations from circular motion (especially an issue for nearby remnants, and for those near $l = 0°$ and $180°$ where the observed velocity does not depend strongly on distance) and ambiguities inside the Solar Circle. Generally, the published errors in kinematic distances are less than $\approx 25\%$, although there are additional possible larger uncertainties depending on whether the (often subjective) association of a particular feature with a remnant is actually correct. A potential bias for statistical studies is that many distance methods are more easily applied to brighter remnants than to fainter ones. This is particularly the case for 21-cm H I absorption studies, which depend on a radio continuum from the remnant being bright, otherwise any absorption could not be studied in reasonable detail. But this also applies to some

Table 2. Galactic SNRs with distance measurements or estimates.

remnant	distance /kpc	method	reference	notes
G4·5+6·8	2.9	optical proper motion/velocity	Blair et al. (1991)	
G6·4−0·1	1.9	H I absorption	Velázquez et al. (2002)	
G11·2−0·3	4.4	H I absorption	Becker et al. (1985)	a,b
G18·8+0·3	14.0	association with CO	Dubner et al. (2004)	
G21·5−0·9	4.6	H I absorption	Davelaar et al. (1986)	a,b
G27·4+0·0	6.8	H I absorption	Sanbonmatsu & Helfand (1992)	
G33·6+0·1	7.8	H I absorption	Frail & Clifton (1989)	a
G34·7−0·4	2.8	H I absorption	Caswell et al. (1975)	a
G39·7−2·0	3.0	association with H I	Dubner et al. (1998)	
G43·3−0·2	10.0	association with H I	Lockhart & Goss (1978)	a
G49·2−0·7	6.0	association with CO	Koo et al. (1995)	
G53·6−2·2	2.8	association with H I	Giacani et al. (1998)	
G55·0+0·3	14.0	association with H I	Matthews et al. (1998)	
G74·0−8·5	0.4	optical proper motion/velocity	Blair et al. (1999)	
G74·9+1·2	6.1	H I column density	Kothes et al. (2003)	
G84·2−0·8	4.5	association with CO	Feldt & Green (1993)	
G89·0+4·7	0.8	association with CO and H I	Tatematsu et al. (1990)	
G93·3+6·9	2.2	H I column density	Foster & Routledge (2003)	
G93·7−0·2	1.5	association with H I	Uyanıker et al. (2002)	
G109·1−1·0	3.0	association with H II region	Kothes et al. (2002)	
G111·7−2·1	3.4	optical proper motion/velocity	Reed et al. (1995)	
G114·3+0·3	0.7	association with H I	Yar-Uyanıker et al (2004)	
G116·5+1·1	1.6	association with H I	Yar-Uyanıker et al (2004)	
G116·9+0·2	1.6	association with H I	Yar-Uyanıker et al (2004)	
G119·5+10·2	1.4	association with H I	Pineault et al. (1993)	
G120·1+1·4	2.3	optical proper motion/velocity	Chevalier et al. (1980)	
G130·7+3·1	3.2	H I absorption	Roberts et al. (1993)	
G132·7+1·3	2.2	association with CO	Routledge et al. (1991)	
G166·0+4·3	4.5	association with H I	Landecker et al. (1989)	
G166·2+2·5	8.0	association with H I	Routledge et al. (1986)	
G184·6−5·8	1.9	various	Trimble (1973)	
G189·1+3·0	1.5	optical absorption	Welsh & Sallmen (2003)	
G205·5+0·5	1.6	various	Odegard (1986)	
G260·4−3·4	2.2	association with H I	Reynoso et al. (1995)	
G263·9−3·3	0.3	pulsar parallax	Caraveo et al. (2001)	
G292·0+1·8	6.0	various	Gaensler & Wallace (2003)	
G292·2−0·5	8.4	H I absorption	Caswell et al. (2004)	
G296·8−0·3	9.6	association with H I	Gaensler et al. (1998a)	
G315·4−2·3	2.3	optical velocity	Sollerman et al. (2003)	
G320·4−1·2	5.2	H I absorption	Gaensler et al. (1999)	
G327·4+0·4	4.8	H I absorption	McClure-Griffiths et al. (2001)	
G327·6+14·6	2.2	optical proper motion/velocity	Winkler et al. (2003)	
G332·4−0·4	3.1	H I absorption	Caswell et al. (1975)	a
G337·0−0·1	11.0	various	Sarma et al. (1997)	
G348·5+0·1	8.0	H I absorption	Caswell et al. (1975)	a
G348·7+0·4	8.0	H I absorption	Caswell et al. (1975)	a
G349·7+0·2	14.8	H I absorption	Caswell et al. (1975)	a

Notes: a) distance recalculated using modern rotation curve; b) see text for further discussion.
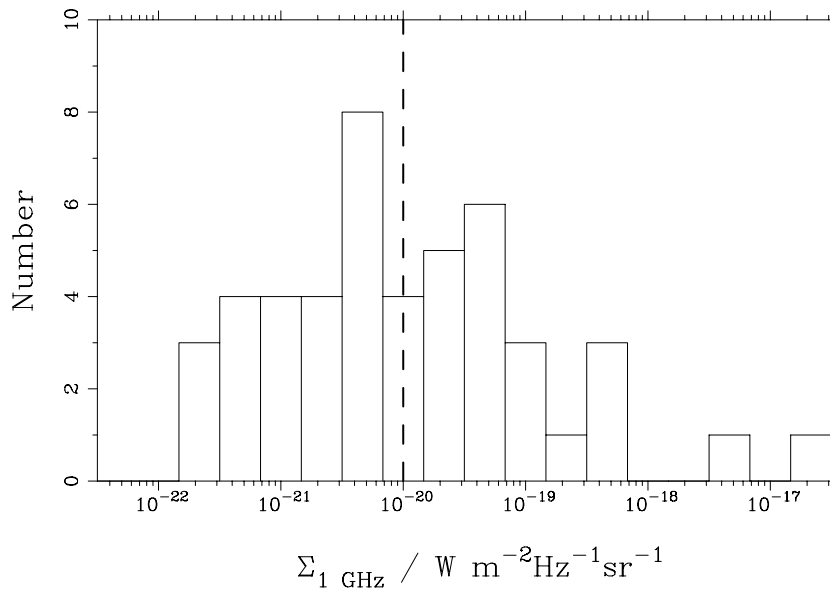
Figure 10. Distribution in surface brightness at 1 GHz of 47 Galactic SNRs with known distances (see Section 5.1). The dashed line indicates the surface brightness completeness limit discussed in Section 3.1.

of the other methods, e.g. association with other H I or CO features in the ISM, where fainter remnants will not be well defined, so that clear morphological association with other features will be more difficult. Indeed, Fig. 10 shows a histogram of the surface brightness of Galactic SNRs with known distances, which shows these tend to be the brighter Galactic SNRs overall (see Fig. 4). Thus, it is likely that, at a given diameter, SNRs with known distances are biased to brighter remnants. The number of SNRs with available distances is sufficiently large that statistical studies – see Section 5.2 – show that the range of intrinsic luminosities of Galactic SNRs is large.

5.2   The $\Sigma-D$ and $L-D$ Relations

Since distances are not available for all SNRs, many statistical studies of Galactic SNRs have relied on the surface-brightness/diameter, or '$\Sigma-D$' relation to derive distances for individual SNRs from their observed flux densities and angular sizes. For remnants with known distances (d), and hence known diameters (D), physically large SNRs are fainter (i.e. they have a lower surface brightness) than small remnants. Using this correlation between Σ and D for remnants with known distances, a physical diameter is deduced from the distance-independent *observed* surface brightness of any remnant. Then a distance to the remnant can be deduced from this diameter and the observed angular size of the remnant.
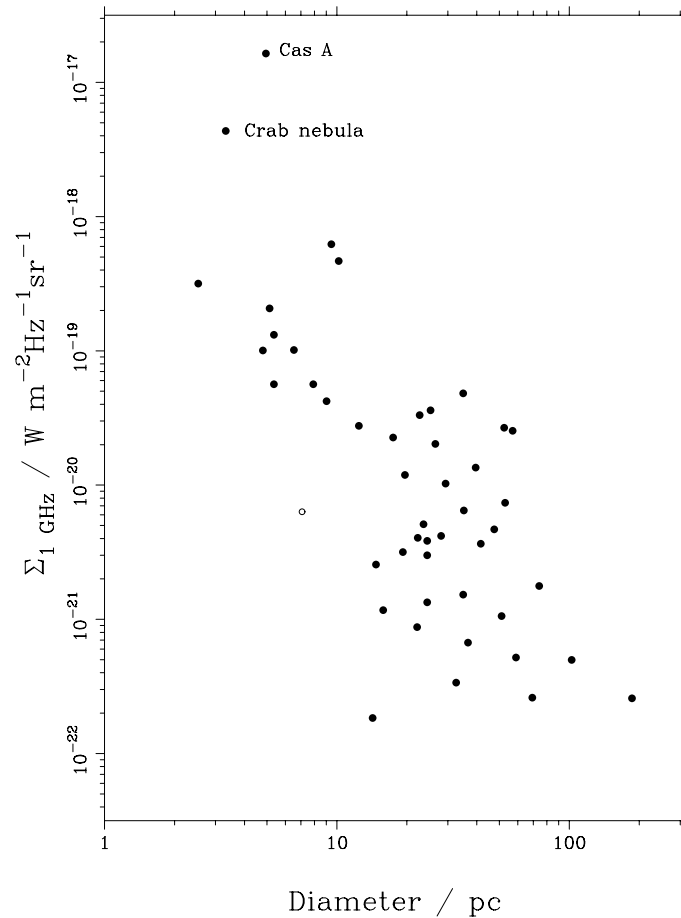
Figure 11. The surface brightness/diameter ($\Sigma{-}D$) relation for 47 Galactic SNRs with known distances (see Table 2), shown as filled circles. The open circle shows the parameters of RX J0852·0−4622 (=G266·2−1·2), if it is at a distance of 200 pc (see text for discussion). Note that the lower left part of this diagram is likely to be seriously affected by selection effects.

The $\Sigma{-}D$ relation for Galactic SNRs with known distances is shown in Fig. 11. As discussed above (Section 5.1), the distances to individual remnants are not homogeneous in quality, and many depend on subjective interpretation of data. Of the SNRs included in this figure, three are 'filled-centre' remnants (the Crab nebula (=G184·6−5·8), 3C58 (=G130·7+3·1) and G74·9+1·2). Nevertheless, Fig. 11 clearly shows a wide range of diameters for a given surface brightness, which is a severe limitation in the usefulness of the $\Sigma{-}D$ relation for deriving the diameters, and hence distances, to individual remnants. For a particular surface brightness, the diameters of SNRs vary by up to about an order of magnitude, or conversely, for a particular diameter, the range of observed surface brightnesses seen varies by more than two orders of magnitude.

D. A. Green
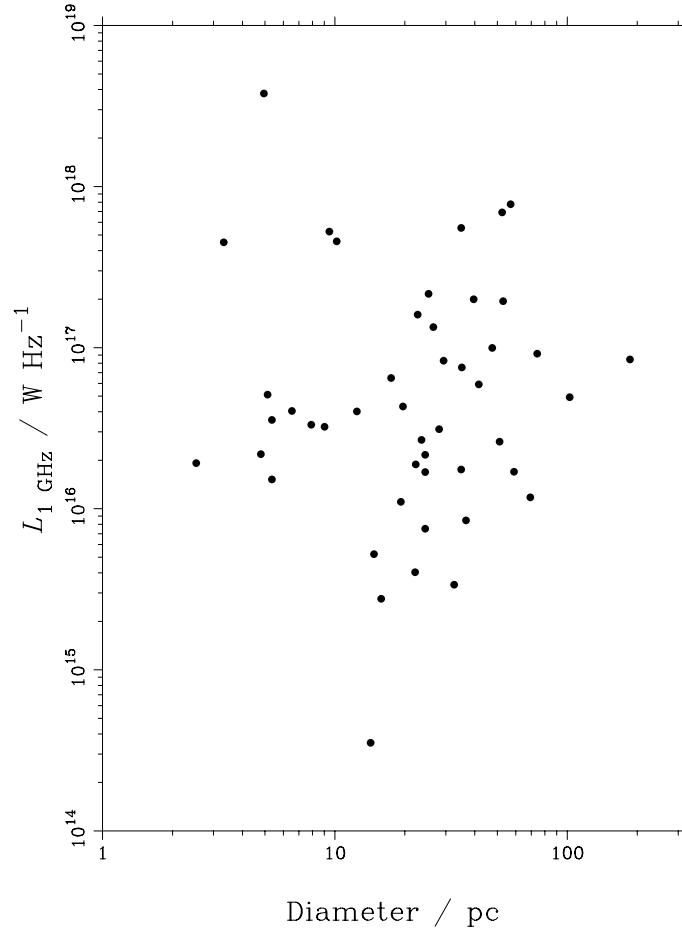
Figure 12. The luminosity/diameter (*L–D*) relation for 47 Galactic SNRs with known distances (see Table 2).

The correlation shown between surface brightness and diameter in Fig. 11 is, however, largely a consequence of the fact that it is a plot of surface-brightness – rather than luminosity – against diameter, *D*. Surface brightness is plotted, because it is the distance-independent observable that is available for (almost) all SNRs, including those for which distances are not available. For remnants whose distances are known, we can instead consider the radio luminosity of the remnants. Since Σ and luminosity, *L*, depends on the flux density *S*, angular size θ, distance *d* and diameter *D*, as

$$\Sigma \propto \frac{S}{\theta^2} \quad \text{and} \quad L \propto S d^2$$

then

$$\Sigma \propto \frac{L}{(\theta d)^2} \quad \text{or} \quad \Sigma \propto \frac{L}{D^2}.$$

Thus, much of the correlation shown in the $\Sigma-D$ relation in Fig. 11 is due to the D^{-2} bias that is inherent when plotting Σ against D, instead of L against D. The $L-D$ relation for Galactic SNRs with known distances in Fig. 12 shows that there is wide range of luminosities for SNRs of all diameters. Cas A is the most luminous Galactic SNR, but it appears to be at the edge of a wide distribution of luminosities. The wide range of luminosities is perhaps not surprising, given that the remnants are produced for a variety of types of supernovae, and that they evolve in regions of ISM with a range of properties (e.g. density), which may well effect the efficiency of the radio emission mechanism at work. For example, some SNRs may initially evolve inside a low-density, wind-blown cavity, and then collide with the much denser regions of the surrounding ISM.

Furthermore, the full range of intrinsic properties of SNRs may be even wider than that shown in Figs 11 and 12, as the selection effects discussed above mean that it is difficult to identify small and/or faint SNRs. One specific example is the recently identified SNR RX J0852·0−4622 (=G266·2−1·2, see Aschenbach 1998), which may extend the range of properties of SNRs considerably (see Duncan & Green 2000). The surface brightness of RX J0852·0−4622 at 1 GHz is $\approx 6 \times 10^{-22}$ W m^{-2} Hz^{-1} sr^{-1}, which places it among the faintest 20 per cent of catalogued remnants. If it is at a distance as small as 200 pc, as suggested by Aschenbach (1998) – see also Redman et al. (2002) – then its diameter would be only 7 pc, see Fig. 11. On the other hand, the deficit of bright, large SNRs in Fig. 11 cannot be explained by any selection effect, and so represents some real limit in the luminosity of remnants at a particular diameter, related to the physics of the underlying radio emission mechanism at work. This upper bound in the $\Sigma-D$ plane can be used to derive an *upper limit* for the diameter of any SNR from its observed surface brightness, and hence an upper limit on its distance. Another upper bound on the distance to any remnant – which may be as useful – is to assume it lies within the Galactic disc.

Case & Bhattacharya (1998) derived a $\Sigma-D$ relation, based on the distances available for 36 remnants – not including filled-centre remnants – from the 1996 version of the catalogue. They argue that it is useful for deriving distances for individual SNRs, with a fractional error of only 0.33, which is very much smaller than the wide range in diameters for a given surface brightness shown in Fig. 11. This optimistic result was only obtained after excluding Cas A from the remnants with known distances used to derived the $\Sigma-D$ relation (as it was deemed to be sufficiently different from other shell SNRs), and also after excluding 7 remnants with high z-values (as three of these showed the largest deviation from the best-fit $\Sigma-D$ relation). It is, however, difficult to decide *a priori* whether a remnant is or is not to be included in the subset of remnants for which Case & Bhattacharya derived distances with relatively small uncertainties.

Also, it is not clear that any best-fit $\Sigma-D$ relation – not withstanding selection effect problems – actually represents the evolutionary track of individual SNRs (see Berkhuijsen 1986). The distribution of SNRs with known distances is a snapshot in time of a population of remnants, and individual remnants may evolve in the $\Sigma-D$ plane in directions quite different from the overall power law fitted to the overall distribution of SNRs (or to the upper limit of the distribution). As a simple example, consider the situation where SNRs have a range of intrinsic luminosities, expand with a constant luminosity up to some particular diameter – which varies for different SNRs depending on their environment (e.g. the surrounding ISM density, which influences their

expansion speed, which may affect the efficiency of radio emission mechanism) – after which their radio luminosity fades rapidly. In this case, the locus of the upper bound to the highest surface brightness remnants for a particular diameter is related to where the luminosities of different SNRs begin to decrease, and does not represent the evolutionary track of any individual remnant. The current direction of the evolutionary track of only one Galactic SNR, Cas A, can be estimated from available observations. The flux density of Cas A is decreasing at approximately 0.8% year^{-1} (Baars et al. 1977; Rees 1990), and its bulk expansion is 0.22% year^{-1} (Agüeros & Green 1999; but see DeLaney et al. 2004 for alternative expansion timescales). These observations suggest Cas A is following a track with $\Sigma \propto D^{-5.6}$, although the uncertainty in this slope is large (nominally ± 1.2, if the uncertainty in the secular flux density decrease is taken as 0.2% year^{-1}, and the expansion timescale of the remnant is between 400 to 500 years).

5.3 An aside: extragalactic selection effects

As noted above, a major problem with statistical studies of Galactic SNRs is the difficulty of obtaining reliable distances for remnants. Studies of samples of remnants in external galaxies are more straightforward in this respect, as all the remnants are at a very similar distance. Given this, then it is arguably more appropriate to consider the $L-D$ relation, rather than the $\Sigma-D$, for extragalactic SNRs – as the latter is not needed to determine distances for individual remnants – with the appropriate selection effects. Then, for unresolved sources, in most radio studies the dominant selection effect is a flux density limit, which corresponds to a fixed luminosity limit for a particular galaxy.

In a recent study of the statistical properties of extragalactic SNRs in several galaxies – in addition to those in the Milky Way – Arbutina et al. (2004) concluded that only in the case of M82 was there a good $L-D$ correlation, and hence a useful $\Sigma-D$ relation also. In other cases there was a poor correlation between the luminosity and diameter of identified SNRs (as noted in Section 5.2 above for Galactic SNRs). However, in their study Arbutina et al. have not correctly appreciated the observational selection effects applicable to the sample of SNRs in M82. This sample of SNRs was identified by Huang et al. (1994) from observations at 8.4 GHz. In Fig. 1 of Arbutina et al. a sensitivity limit corresponding to a luminosity of $\approx 7 \times 10^{24}$ erg s^{-1} Hz^{-1} is plotted, which although appropriate at 8.4 GHz, is not appropriate for the luminosities of the M82 sample of SNRs plotted in this figure, which are at 1 GHz. The true luminosity limit from Huang et al.'s observations should be moved upwards on Arbutina et al.'s Fig. 1 by ≈ 3 (i.e. $\approx 8.4^{0.5}$ for a typical spectral index of 0.5 to correct from 8.4 to 1 GHz). Moreover, the actual observational selection effects provide a more stringent limit on the detectable luminosities of the larger SNRs in the sample. Any remnants with a diameter of larger than ≈ 3 pc were resolved by Huang et al.'s observations, and a surface brightness limit (equivalent to luminosity scaling as D^2), not a constant luminosity limit is appropriate (see Fig. 2 of Huang et al., who show these limits on a $\Sigma-D$ rather than a $L-D$ plot). Consequently, the apparent range of luminosities of SNRs in M82 is strongly limited by selection effects, particularly for the larger remnants. Indeed, it is noticeable that the range of luminosities shown for the larger remnants in M82 appears smaller than that of the smaller remnants, which seems unlikely to be real. Thus the range of luminosities

of SNRs in M82 is likely to extend to lower values, but these objects have not been identified due to selection effects. In this case the correlation between luminosity and diameter for remnants here is not strong, as is the case in other galaxies, including our own. Consequently, the $\Sigma-D$ relation for M82 is also affected by selection effects, and is therefore of limited use.

6. Galactic SNR distribution

The distribution of SNRs in the Galaxy is of interest for many astrophysical studies, particularly in relation to their energy input into the ISM and for comparison with the distributions of possible progenitor populations. Such studies are, however, not straightforward, due to observational selection effects and the lack of reliable distance estimates available for most identified remnants. In particular, all SNRs in the anti-centre (i.e. 2nd and 3rd Galactic quadrants) are outside the Solar Circle, at large Galactocentric radii, in regions where the background Galactic emission is low, so that low surface brightness remnants are relatively easy to identify (see Section 3). Without taking selection effects into account, the larger number of fainter SNRs in the anti-centre leads to an apparently broad distribution of Galactic SNRs in Galactocentric radius (e.g. the very broad distribution of SNRs derived by Li et al. (1991), who included all SNRs in their analyses). A more complicated method to derive the radial distribution of Galactic SNRs is that used by Case & Bhattacharya (1996, 1998), following a method used by Narayan (1987) for pulsars. This relies on (i) assuming catalogues of Galactic SNRs are complete for SNRs within a distance of 3 kpc; (ii) using $\Sigma-D$ derived distances for the SNRs, and (iii) attempts to correct for observational selection effects using a scaling factor that varies in many bins across the disc of the Galaxy. However, this is difficult given the uncertainties in the usefulness of $\Sigma-D$ relation discussed above, and the necessity of deconvolving selection effects from the observed distribution of SNRs. An alternative approach is to investigate the distribution of SNRs in Galactic coordinates, restricting the studies to relatively bright remnants, for which current catalogues are thought to be complete. van den Bergh (1988a,b) discussed the distribution of observed SNRs and noted that high surface brightness remnants (in this case taken to be $\Sigma_{1\,\mathrm{GHz}} > 3 \times 10^{-21}$ W m^{-2} Hz^{-1} sr^{-1}) are concentrated in a thin nuclear disc when plotted in Galactic coordinates. As noted by Fürst's comments to van den Bergh (1988b), this conclusion is strengthened by a more realistic surface brightness completeness limit.

More quantitatively – following the method of Li et al., but using an appropriate selection brightness cut-off – the observed distribution of bright SNRs with Galactic longitude can be compared with that expected from various models. A major advantage of this method is that it avoids the problem that we lack accurate distances to individual SNRs, although on the other hand it uses only a sub-set of the known Galactic SNRs. Fig. 13 shows the observed distributions with Galactic longitude of all Galactic SNRs, and of the 64 remnants which have $\Sigma_{1\,\mathrm{GHz}} > 10^{-20}$ W m^{-2} Hz^{-1} sr^{-1} (this is a similar number to the 71 remnants used in a similar study presented in Green 1996a, which used a slightly lower surface brightness cut-off applied to the SNR catalogue of Green 1996b). By applying the surface brightness cut-off, so that the surface brightness selection effect is not important, it is clear that the distribution of Galactic remnants is actually much more concentrated towards $l = 0°$ than if all remnants are considered (cf. Fig. 5). Fig. 13

D. A. Green

a) all SNRs

b) high surface brightness SNRs

Galactic longitude l
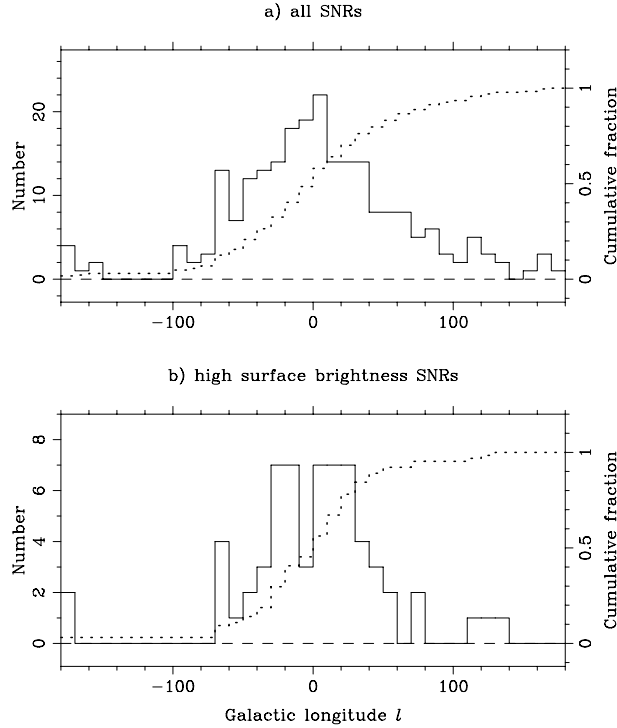
Figure 13. The distribution in Galactic longitude of (top) all 231 Galactic SNRs, and (bottom) the 64 high surface brightness SNRs with $\Sigma_{1\,\mathrm{GHz}} > 10^{-20}\,\mathrm{W\,m^{-2}\,Hz^{-1}\,sr^{-1}}$. Each plot shows as a solid line a histogram of the observed longitudes of the remnants (left scale), and as a dotted line for cumulative fraction (right scale).

shows evidence for a deficit of SNRs near $l = 350°$, which may be a true deficit if there is a decrease in the space density of SN progenitors towards the Galactic centre. However, it may also be, in part at least, due to the difficulty of finding remnants in this region of the Galactic plane, due to the very complex background emission and confusing Galactic sources (e.g. H II regions). Any remaining incompleteness in current catalogues, both for the surface brightness and angular diameter selection effects, are expected to be worse closer to $b = 0°$ (because of the increased confusion in the case of the surface brightness selection effect, and the longer line-of-sight through the Galaxy for missing small, i.e. young but distant remnants). Thus, the true distribution in l is likely to be somewhat *narrower* than is indicated in Fig. 13. For comparison with the observed distributions in Galactic longitude, simple Monte Carlo models of the distribution of SNRs in the disc of the Galaxy were constructed assuming a simple, circularly symmetric, Gaussian distribution, where the probability distribution varies with Galactocentric radius, R, as

$$\propto e^{-(R/\sigma)^2},$$

(where σ is the Gaussian Galactocentric scale length, assuming the distance to the Galactic Centre

5.0 kpc scale length

6.5 kpc scale length
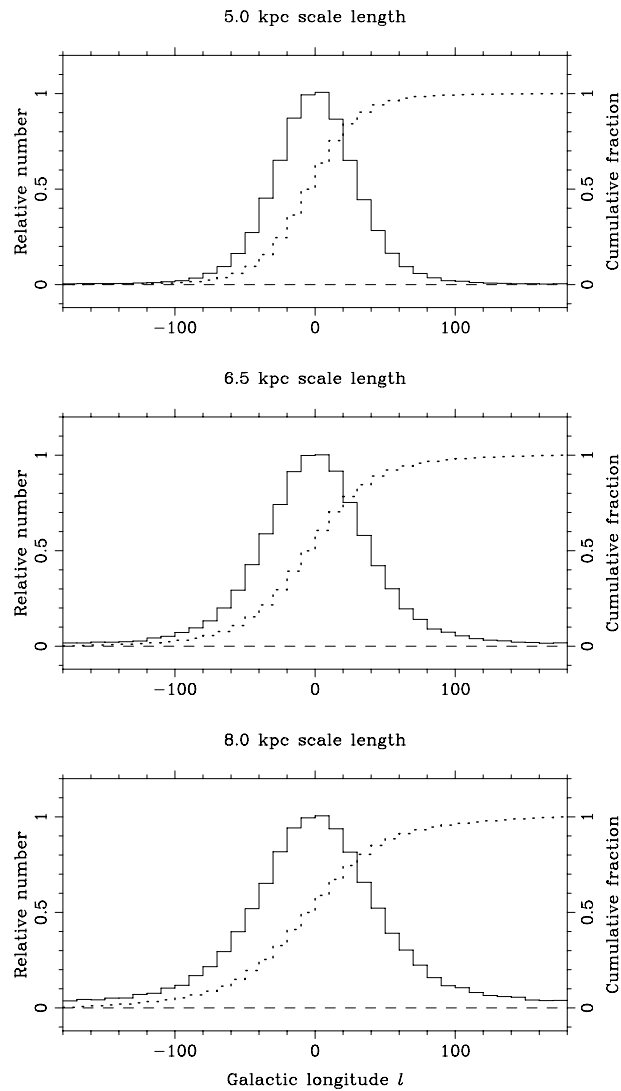
8.0 kpc scale length

Figure 14. Model distribution in Galactic longitude of Gaussian distributions of SNRs with three different Galactocentric radius scale lengths (cf. the observed distribution in Fig. 13).

is 8.5 kpc). Fig. 14 shows plots of the expected distribution of SNRs in Galactic longitude of three such models for different scale lengths. As noted above, the true distribution is likely to be somewhat narrower than that derived from the observations, due to residual selection effects, so that this scale length is an upper limit. A χ^2 comparison of the observed and model cumulative distributions indicates that for this simple model, a scale length of $\approx$ 6.5 kpc best matches the observed distribution of high brightness SNRs.

The model distribution of SNRs derived above should, however, be interpreted cautiously, as not only is it a simplistic model without spiral arm structures, but also it is a model of the distribution of *observed* remnants. It is far from clear what factors affect the brightness and lifetime of appreciable radio emission from SNRs – i.e. their observability at radio wavelengths – and hence how close the distribution of observed SNRs is to the parent supernovae distribution. The distribution of SNRs could reflect the distribution of, for example, the density of the ISM, or the Galactic magnetic field, if these are important factors in determining the brightness and lifetime of radio emission from SNRs.

7. Conclusions

Here I have presented a recent catalogue of 231 Galactic SNRs, and have discussed the selection effects that apply to the identification of remnants. Both surface brightness and angular size selection effects are important, and these need to be borne in mind when statistical studies of Galactic SNRs are made. One consequence of the current angular size selection effect is that few young but distant remnants have yet been identified in the Galaxy. These objects are likely to be in complex regions of the Galactic plane, and further observations – using a wide range of radio wavelengths and/or the combination of radio and other wavelengths – are required to identify these missing objects. For remnants with known distances, the intrinsic range of luminosity of Galactic SNRs is large, which combined with selection effects, means that the $\Sigma - D$ relation is of limited use for determining distances to individual remnants, or for statistical studies.

Acknowledgements

References

Agüeros M., Green D. A., 1999, *MNRAS*, **305**, 957.
Arbutina B., Urošević D., Stanković M., Tešić Lj., 2004, *MNRAS*, **350**, 346.
Arendt R. G., 1989, *ApJS*, **70**, 181.
Aschenbach B., 1998, *Nature*, **396**, 141.
Baars J. W. M., Genzel R., Pauliny-Toth I. I. K., Witzel, A., 1977, *A&A*, **61**, 99.
Becker R. H., Markert T., Donahue M., 1985, *ApJ*, **296**, 461.
Berkhuijsen E. M., 1973, *A&A*, **24**, 143.
Berkhuijsen E. M., 1986, *A&A*, **166**, 257.
Blair W. P., Long K. S., Vancura O., 1991, *ApJ*, **366**, 484.

Blair W. P., Sankrit R., Raymond J. C., Long K. S., 1999, *AJ*, **118**, 942.

Braje T. M., Romani R. W., Roberts M. S. E., Kwai N., 2002, *ApJ*, **565**, L91.

Brogan C. L., Devine K. E., Lazio T. J., Kassim N. E., Tam C. R., Brisken W. F., Dyer K. K., Roberts M. S. E., 2004, *AJ*, **127**, 355

Camilo F., Lorimer D. R., Bhat, N. D. R., Gotthelf E. V., Halpern J. P., Wang Q. D., Lu F. J., Mirabal N., 2002, *ApJ*, **574**, L71.

Cappellaro M., 2003, in *Supernovae and Gamma-Ray Bursters*, Lecture Notes in Physics, Volume 598, ed K. W. Weiler, Springer, Berlin, p. 21.

Caraveo P. A., De Luca A., Mignani R. P., Bignami G. F., 2001, *ApJ*, **561**, 930.

Case G. L., Bhattacharya D., 1996, *A&AS*, **120**, 437.

Case G. L., Bhattacharya D., 1998, *ApJ*, **504**, 761.

Caswell J. L., Murray J. D., Roger R. S., Cole D. J., Cooke D. J., 1975, *A&A*, **45**, 239.

Caswell J. L., McClure-Griffiths N. M., Cheung M. C. M., 2004, *MNRAS*, **352**, 1405.

Chevalier R. A., Kirshner R. P., Raymond J. C., 1980, *ApJ*, **235**, 186.

Cohen M., Green A. J., 2001, *MNRAS*, **325**, 531.

Combi J. A., Testori J. C., Romero G. E., Colomb F. R., 1995, *A&A*, **296**, 514.

Condon J. J., Griffith M. R., Wright A. E., 1993, *AJ*, **106**, 1095.

Condon J. J., Cotton W. D., Greisen E. W., Yin Q. F., Perley R. A., Taylor G. B., Broderick J. J., 1998, *AJ*, **115**, 1693.

Davelaar J., Smith A., Becker R. H., 1986, *ApJ*, **300**, L59.

DeLaney T., Rudnick L., Fesen R. A., Jones T. W., Petre R., Morse J. A., 2004, *ApJ*, **613**, 343.

Dubner G. M., Holdaway M., Goss W. M., Mirabel I. F., 1998, *AJ*, **116**, 1842.

Dubner G., Giacani E., Reynoso E., Parón S., 2004, *A&A*, **426**, 201.

Duncan A. R., Green D. A., 2000, *A&A*, **364**, 732.

Duncan A. R., Stewart R. T., Haynes R. F., Jones K. L., 1995, *MNRAS*, **277**, 36.

Duncan A. R., Stewart R. T., Haynes R. F., Jones K. L., 1997, *MNRAS*, **287**, 722.

Feldt C., Green D. A., 1993, *A&A*, **274**, 421.

Fesen R. A., Hurford A. P., 1996, *ApJS*, **106**, 563.

Filipović M. D., Stupar M., Jones P. A., White G. L., 2002, in *Neutron Stars in Supernova Remnants*, ASP Conference Series, Volume 271, eds P. O. Slane & B. M. Gaensler, ASP, San Francisco, p. 387.

Foster T., Routledge D., 2003, *ApJ*, **598**, 1005.

Frail D. A., Clifton T. R., 1989, *ApJ*, **336**, 854.

Fürst E., Reich W., Reich P., Reif K., 1990, *A&AS*, **85**, 691.

Gaensler B. M., Wallace B. J., 2003, *ApJ*, **594**, 326.

Gaensler B. M., Manchester R. N., Green A. J., 1998a, *MNRAS*, **296**, 813.

Gaensler B. M., Stappers B. W., Frail D. A., Johnston S., 1998b, *ApJ*, **499**, L69.

Gaensler B. M., Brazier K. T. S., Manchester R. N., Johnston S., Green A. J., 1999, *MNRAS*, **305**, 724.

Gaensler B. M., Schulz N. S., Kaspi V. M., Pivavaroff M. J., Becker W. E., 2003, *ApJ*, **588**, 441.

Giacani E. B., Dubner G., Cappa C., Testori J., 1998, *A&AS*, **133**, 61.

Giacani E. B., Frail D. A., Goss W. M., Vieytes M., 2001, *AJ*, **121**, 3133.

Green A. J., 2002, in *The Universe at Low Radio Frequencies*, IAU Symposium 199, eds A. Pramesh Rao, G. Swarup & Gopal Krishna, ASP, San Francisco, p. 259.

Green A. J., Cram L. E., Large M. I., Ye T. S., 1999, *ApJS*, **122**, 207.

Green D. A., 1984, *MNRAS*, **209**, 449.

Green D. A., 1985, *MNRAS*, **216**, 691.

Green D. A., 1988, *Ap&SS*, **148**, 3.

Green D. A., 1989, *AJ*, **98**, 1358.

Green D. A., 1991, *PASP*, **103**, 209.

Green D. A., 1996a, in *Supernovae and Supernova Remnants*, IAU Colloquium 145, eds R. McCray & Z. Wang, Cambridge University Press, p. 341.

Green D. A., 1996b, in *Supernovae and Supernova Remnants*, IAU Colloquium 145, eds R. McCray & Z. Wang, Cambridge University Press, p. 419.

Green D. A., 2001a, in *High Energy Gamma-Ray Astronomy*, eds F. A. Aharonian & H. J. Völk, American Institute of Physics, Melville, New York, p. 59.

Green D. A., 2001b, *MNRAS*, **326**, 283.

Green D. A., Gull S. F., 1984, *Nature*, **312**, 527.

Helfand D. J., Chance D., Becker R. H., White R. L., 1984, *AJ*, **89**, 819.

Huang Z. P., Thuan T. X., Chevalier R. A., Condon J. J., Yin Q. F., 1994, *ApJ*, **424**, 114.

Jones D. H., Stappers B. W., Gaensler B. M., 2002, *A&A*, **389**, L1.

Kassim N. E., 1989, *ApJS*, **71**, 799.

Kim K.-T., Koo B.-C., 2000, *ApJ*, **529**, 229.

Koo B.-C., Heiles C., 1991, *ApJ*, **382**, 204.

Koo B., Kim K., Seward F. D., 1995, *ApJ*, **447**, 211.

Kothes R., Landecker T. L., Foster T., Leahy D. A., 2001, *A&A*, **376**, 641.

Kothes R., Uyanıker B., Yar A., 2002, *ApJ*, **576**, 169.

Kothes R., Reich W., Foster T., Byun D., 2003, *ApJ*, **588**, 852.

Kovalenko A. V., Pynzar' A. V., Udal'tsov V. A., 1994, *Astronomy Reports*, **38**, 95.

Landecker T. L., Pineault S., Routledge D., Vaneldik J. F., 1989, *MNRAS*, **237**, 277.

Langston G., Minter A., D'Addario L., Eberhart K., Koski K., Zuber J., 2000, *AJ*, **119**, 2801.

Li Z.-W., Wheeler J. C., Bash F. N., Jefferys W. H., 1991, *ApJ*, **378**, 93

Lockhart I. A., Goss W. M., 1978, *A&A*, **67**, 355.

Lockman F. J., Stil J. M., 2004, in *Milky Way Surveys: The Structure and Evolution of our Galaxy*, ASP Conference Series 317, eds D. Clemens, R. Shah & T. Brainerd, in press (`astro-ph/0310762`).

Lum K. S. K., Canizares C. R., Clark S. W., Coyne J. M., Markert T. H., Saez P. J., Schattenburg M. L., Winkler P. F., 1992, *ApJS*, **78**, 423.

McClure-Griffiths N. M., 2002, in *Seeing Through the Dust: Interstellar Medium in Galaxies*, ASP Conference Series 276, eds A. R. Taylor, T. L. Landecker & A. Willis, ASP, San Francisco, p. 58

McClure-Griffiths N. M., Green A. J., Dickey J. M., Gaensler B. M., Haynes R. F., Wieringa M. H., 2001, *ApJ*, **551**, 394.

Maciejewski W., Murphy E. M., Lockman F. J., Savage B. D., 1996, *ApJ*, **469**, 238.

Matthews B. C., Wallace B. J., Taylor A. R., 1998, *ApJ*, **493**, 312.

Misanovic Z., Cram L., Green A., 2002, *MNRAS*, **335**, 114.

Narayan R., 1987, *ApJ*, **319**, 162.

Normandeau M., Taylor A. R., Dewdney P. E., Basu S., 2000, *AJ*, **119**, 2982.

Odegard N., 1986, *ApJ*, **301**, 813.

Pineault S., Landecker T. L., Madore B., Gaumont-Guay S., 1993, *AJ*, **105**, 1060.

Redman M. P., Meaburn J., Bryce M., Harman D. J., O'Brien T. J., 2002, *MNRAS*, **336**, 1039.

Reed J. E., Hester J. J., Fabian A. C., Winkler P. F., 1995, *ApJ*, **440**, 706.

Rees N., 1990, *MNRAS*, **243**, 637.

Reich W., Fürst E., Altenhoff W. J., Reich P., Junkes N., 1985, *A&A*, **151**, L10

Reich W., Fürst E., Reich P., Junkes N., 1988, in *Supernova Remnants and the Interstellar Medium*, IAU Colloquium 101, eds R. S. Roger & T. L. Landecker, Cambridge University Press, p. 293.

Reich W., Fürst E., Reich P., Reif K., 1990, *A&AS*, **85**, 633.

Reynoso E. M., Dubner G. M., Goss W. M., Arnal E. M., 1995, *AJ*, **110**, 318.

Rho J., Petre R., 1998, *ApJ*, **503**, L167.

Roberts D. A., Goss W. M., Kalberla P. M. W., Herbstmeier U., Schwarz U. J., 1993, *A&A*, **274**, 427.

Routledge D., Landecker T. L., Vaneldik J. F., 1986, *MNRAS*, **221**, 809.

Routledge D., Dewdney P. E., Landecker T. L., Vaneldik J. F., 1991, *A&A*, **247**, 529.

Safi-Harb S., Harrus I. M., Petre R., Pavlov G. G., Koptsevich A. B., Sanwal D., 2001, *ApJ*, **561**, 308.

Saikia D. J., Thomasson P., Roy S., Pedlar A., Muxlow T. W. B., 2004, *MNRAS*, **354**, 827.

Saken J. M., Fesen R. A., Shull J. M., 1992, *ApJS*, **81**, 715.

Sanbonmatsu K. Y., Helfand D. J., 1992, *AJ*, **104**, 2189.

Sarma A. P., Goss W. M., Green A. J., Frail D. A., 1997, *ApJ*, **483**, 335.

Schaudel D., Becker W., Aschenbach B., Trümper J., Reich W., Weisskopf M., 2002, in *Neutron Stars, Pulsars and Supernova Remnants*, eds W. Becker, H. Lesch & J. Trümper, MPE Report 278, p. 26.

Seward F. D., 1990, *ApJS*, **73**, 781.

Sollerman J., Ghavamian P., Lundqvist P., Smith R. C., 2003, *A&A*, **407**, 249.

Sramek R. A., Cowan J. J., Roberts D. A., Goss W. M., Ekers R. D., 1992, *AJ*, **104**, 704.

Stephenson F. R., Green D. A., 2002, *Historical Supernovae and their Remnants*, Oxford University Press.

Stil J. M., Irwin J. A., 2001, *ApJ*, **563**, 816.

Stothers R., Frogel J. A., 1974, *AJ*, **79**, 456.

Strom R. G., 1994, *A&A*, **288**, L1.

Tatematsu K., Fukui Y., Landecker T. L., Roger R. S., 1990, *A&A*, **237**, 189.

Taylor A. R., Gibson S. J., Peracaula M., Martin P. G.; Landecker T. L., Brunt C. M., Dewdney P. E., Dougherty S. M., Gray A. D., Higgs L. A., Kerton C. R., Knee L. B. G., Kothes R., Purton C. R., Uyanıker B., Wallace B. J., Willis A. G., Durand D., 2003, *AJ*, **125**, 3145.

Trimble V., 1973, *PASP*, **85**, 579.

Trushkin S. A., 1998, *Bull. Special Astrophys. Obs.*, **46**, 62.

Uyanıker B., Kothes R., 2002, *ApJ*, **574**, 805.

Uyanıker B., Kothes R., Brunt C. M., 2002, *ApJ*, **565**, 1022.

van den Bergh S., 1988a, *PASP*, **100**, 205.

van den Bergh S., 1988b, in *Supernova Shells and Their Birth Events*, ed. W. Kundt, Springer-Verlag, Berlin, p. 44.

Velázquez P. F., Dubner G. M., Goss W. M., Green A. J., 2002, *AJ*, **124**, 2145.

Welsh B. Y., Sallmen S., 2003, *A&A*, **408**, 545.

Whiteoak J. B. Z., Green A. J., 1996, *A&AS*, **118**, 329.

Winkler P. F., Gupta G., Long K. S., 2003, *ApJ*, **585**, 324.

Woermann B., Gaylard M. J., Otrupcek R., 2001, *MNRAS*, **325**, 1213.

Yar-Uyanıker A., Uyanıker B., Kothes R., 2004, *ApJ*, in press (`astro-ph/0408386`).

A. The Galactic SNR catalogue: 2004 January version

This appendix presents a catalogue of Galactic supernova remnants. This catalogue is an updated version of those presented in detail in Green (1984, 1988) and in summary form in Green (1991, 1996b) and Stephenson & Green (2002). Detailed versions of this catalogue have been made available on the World-Wide-Web since 1993 November (with subsequent versions of 1995 July, 1996 August, 1998 September, 2000 August, 2001 December and 2004 January). This, the 2004 January version of the catalogue, contains 231 SNRs. The detailed version of this catalogue is available at

`http://www.mrao.cam.ac.uk/surveys/snrs/`

which contains over a thousand references for the individual SNRs.

For each remnant in the catalogue the following parameters are given.

- **Galactic Coordinates** of the source centroid, quoted to the nearest tenth of a degree as is conventional. (Note: in this catalogue additional leading zeros are not used.)

- **Right Ascension** and **Declination** of the source centroid. The accuracy of the quoted values depends on the size of the remnant, for small remnants they are to the nearest few seconds of time and the nearest minute of arc respectively, whereas for larger remnants they are rounded to coarser values, but are in every case sufficient to specify a point within the boundary of the remnant. These coordinates are almost always deduced from radio maps rather than from X-ray or optical observations, and are for J2000.0.

- **Angular Size** of the remnant, in arcminutes, usually taken from the highest resolution radio map available. The boundary of most remnants approximates reasonably well to a circle or an ellipse, a single value is quoted for the angular size of the more nearly circular remnants, which is the diameter of a circle with an area equal to that of the remnant, but for elongated remnants the product of two values is quoted, and these are the major and minor axes of the remnant boundary modelled as an ellipse. In a few cases an ellipse is not a satisfactory description of the boundary of the object (refer to the description of the individual object given in its catalogue entry), although an angular size is still quoted for information. For 'filled-centre' remnants the size quoted is for the largest extent of the observed radio emission, not, as at times has been used by others, the half-width of the centrally brightened peak.

- **Type** of the SNR: 'S' or 'F' if the remnant shows a 'shell' or 'filled-centre' structure, or 'C' if it shows 'composite' (or 'combination') radio structure with a combination of shell and filled-centre characteristics; or 'S?', 'F?' or 'C?', respectively, if there is some uncertainty, or '?' in several cases where an object is conventionally regarded as an SNR even though its nature is poorly known or not well understood. (Note: the term 'composite' has been used in a different sense by some authors, to describe SNRs with shell radio and centrally-brightened X-ray morphologies. An alternative term used to describe such remnants is 'mixed morphology', see Rho & Petre 1998.)

- **Flux Density** of the remnant at 1 GHz in jansky. This is *not* a measured value, but is deduced from the observed radio frequency spectrum of the source. The frequency of 1 GHz is chosen because flux density measurements at frequencies both above and below this value are usually available.

- **Spectral Index** of the integrated radio emission from the remnant, α (here defined in the sense, $S \propto \nu^{-\alpha}$, where S is the flux density at a frequency ν), either a value that is quoted in the literature, or one deduced from the available integrated flux densities of the remnant. For several SNRs a simple power law is not adequate to describe their radio spectra, either because there is evidence that the integrated spectrum is curved or the spectral index varies across the face of the remnant. In these cases the spectral index is given as 'varies' (refer to the description of the remnant and appropriate references in the detailed catalogue entry

for more information). In some cases, for example where the remnant is highly confused with thermal emission, the spectral index is given as '?' since no value can be deduced with any confidence.

- **Other Names** that are commonly used for the remnant. These are given in parentheses if the remnant is only a part of the source. For some remnants, notably the Crab nebula, not all common names are given.

A summary of the data available for all 231 remnants in the catalogue is given in Table A1.

In the detailed listings, available on the World-Wide-Web, notes on a variety of topics are given for each remnant. First, it is noted if other Galactic coordinates have at times been used to label it (usually before good observations have revealed the full extent of the object), if the SNR is thought to be the remnant of a historical SN, or if the nature of the source as an SNR has been questioned (in which case an appropriate reference is usually given later in the entry). Brief descriptions of the remnant from the available radio, optical and X-ray observations as applicable are then given, together with notes on available distance determinations, and any point sources or pulsars in or near the object (although they may not necessarily be related to the remnant). Finally, appropriate references to observations are given for each remnant, complete with journal, volume, page, and a short description of what information each paper contains (for radio observations these include the telescopes used, the observing frequencies and resolutions, together with any flux density determinations). These references are *not* complete, but cover representative and recent observations of the remnant – up to the end of 2003 – and they should themselves include references to earlier work. The references do not generally include large observational surveys – of particular interest in this respect are: the Effelsberg 100-m survey at 2.7 GHz of the Galactic plane $358° < l < 240°$, $|b| < 5°$ by Reich et al. (1990) and Fürst et al. (1990), reviews of the radio spectra of some SNRs by Kassim (1989), Kovalenko, Pynzar' & Udal'tsov (1994) and Trushkin (1998), the Parkes 64-m survey at 2.4 GHz of the Galactic plane $238° < l < 365°$, $|b| < 5°$ by Duncan et al. (1995) and Duncan et al. (1997), the Molonglo Galactic plane survey at 843 MHz of $245° < l < 355°$, $|b| < 1°\!.5$ by Green et al. (1999), the survey of $345° < l < 255°$, $|b| < 5°$ at 8.35 and 14.35 GHz by Langston et al. (2000), reviews of *Einstein* X-ray imaging and spectroscopic observations of Galactic SNRs by Seward (1990) and Lum et al. (1992) respectively, surveys of *IRAS* observations of SNRs and their immediate surroundings by Arendt (1989) and by Saken, Fesen & Shull (1992), the survey of H I emission towards SNRs by Koo & Heiles (1991), and the catalogue by Fesen & Hurford (1996) of UV/optical/infra-red lines identified in SNRs. The detailed version of the catalogue also including notes on the objects no longer thought to be SNRs, and on many possible and probable remnants in the literature. It should also be noted that: (i) some radio continuum and H I loops in the Galactic plane (e.g. Berkhuijsen 1973) may be parts of very large, old SNRs, but they have not been included in the catalogue (see also Combi et al. 1995; Maciejewski et al. 1996; Kim & Koo 2000; Normandeau et al. 2000; Woermann, Gaylard & Otrupcek 2001; Stil & Irwin 2001; Uyanıker & Kothes 2002), (ii) the distinction between filled-centre remnants and pulsar wind nebula is not clear, and isolated, generally faint, pulsar wind nebulae are also not included in the catalogue (e.g. Gaensler et al. 1998b; Giacani et al. 2001; Jones, Stappers & Gaensler 2002; Braje et al. 2002; Gaensler et al. 2003).

D. A. Green

Table A1. Galactic Supernova Remnants: summary data.

l	*b*	RA (J2000) Dec (h m s) (° ′)	size /arcmin	type	Flux at 1 GHz/Jy	spectral index	other name(s)
0.0	+0.0	17 45 44 −29 00	3.5 × 2.5	S	100?	0.8?	Sgr A East
0.3	+0.0	17 46 15 −28 38	15 × 8	S	22	0.6	
0.9	+0.1	17 47 21 −28 09	8	C	18?	varies	
1.0	−0.1	17 48 30 −28 09	8	S	15	0.6?	
1.4	−0.1	17 49 39 −27 46	10	S	2?	?	
1.9	+0.3	17 48 45 −27 10	1.2	S	0.6	0.7	
3.7	−0.2	17 55 26 −25 50	14 × 11	S	2.3	0.65	
3.8	+0.3	17 52 55 −25 28	18	S?	3?	0.6	
4.2	−3.5	18 08 55 −27 03	28	S	3.2?	0.6?	
4.5	+6.8	17 30 42 −21 29	3	S	19	0.64	Kepler, SN1604, 3C358
4.8	+6.2	17 33 25 −21 34	18	S	3	0.6	
5.2	−2.6	18 07 30 −25 45	18	S	2.6?	0.6?	
5.4	−1.2	18 02 10 −24 54	35	C?	35?	0.2?	Milne 56
5.9	+3.1	17 47 20 −22 16	20	S	3.3?	0.4?	
6.1	+1.2	17 54 55 −23 05	30 × 26	F	4.0?	0.3?	
6.4	−0.1	18 00 30 −23 26	48	C	310	varies	W28
6.4	+4.0	17 45 10 −21 22	31	S	1.3?	0.4?	
7.0	−0.1	18 01 50 −22 54	15	S	2.5?	0.5?	
7.7	−3.7	18 17 25 −24 04	22	S	11	0.32	1814−24
8.7	−5.0	18 24 10 −23 48	26	S	4.4	0.3	
8.7	−0.1	18 05 30 −21 26	45	S?	80	0.5	(W30)
9.8	+0.6	18 05 08 −20 14	12	S	3.9	0.5	
11.2	−0.3	18 11 27 −19 25	4	C	22	0.6	
11.4	−0.1	18 10 47 −19 05	8	S?	6	0.5	
12.0	−0.1	18 12 11 −18 37	7?	?	3.5	0.7	
13.3	−1.3	18 19 20 −18 00	70 × 40	S?	?	?	
13.5	+0.2	18 14 14 −17 12	5 × 4	S	3.5?	1.0?	
15.1	−1.6	18 24 00 −16 34	30 × 24	S	5.5?	0.8?	
15.9	+0.2	18 18 52 −15 02	7 × 5	S?	5	0.6?	
16.2	−2.7	18 28 50 −16 11	17	S	2	0.5	
16.7	+0.1	18 20 56 −14 20	4	C	3.0	0.6	
16.8	−1.1	18 25 20 −14 46	30 × 24?	?	2?	?	
17.4	−2.3	18 30 55 −14 52	24?	S	4.8?	0.8?	
17.8	−2.6	18 32 50 −14 39	24	S	4.0?	0.3?	
18.8	+0.3	18 23 58 −12 23	17 × 11	S	33	0.4	Kes 67

Table A1. (continued).

l	b	RA (J2000) Dec (h m s) (° ′)	size /arcmin	type	Flux at 1 GHz/Jy	spectral index	other name(s)
18.9	−1.1	18 29 50 −12 58	33	C?	37	varies	
20.0	−0.2	18 28 07 −11 35	10	F	10	0.0	
21.5	−0.9	18 33 33 −10 35	4	C	6?	0.0	
21.8	−0.6	18 32 45 −10 08	20	S	69	0.5	Kes 69
22.7	−0.2	18 33 15 −09 13	26	S?	33	0.6	
23.3	−0.3	18 34 45 −08 48	27	S	70	0.5	W41
23.6	+0.3	18 33 03 −08 13	10?	?	8?	0.3	
24.7	−0.6	18 38 43 −07 32	15?	S?	8	0.5	
24.7	+0.6	18 34 10 −07 05	30 × 15	C?	20?	0.2?	
27.4	+0.0	18 41 19 −04 56	4	S	6	0.68	4C−04.71
27.8	+0.6	18 39 50 −04 24	50 × 30	F	30	varies	
28.6	−0.1	18 43 55 −03 53	13 × 9	S	3?	?	
28.8	+1.5	18 39 00 −02 55	100?	S?	?	0.4?	
29.6	+0.1	18 44 52 −02 57	5	S	1.5?	0.5?	
29.7	−0.3	18 46 25 −02 59	3	C	10	0.7	Kes 75
30.7	−2.0	18 54 25 −02 54	16	?	0.5?	0.7?	
30.7	+1.0	18 44 00 −01 32	24 × 18	S?	6	0.4	
31.5	−0.6	18 51 10 −01 31	18?	S?	2?	?	
31.9	+0.0	18 49 25 −00 55	7 × 5	S	24	0.55	3C391
32.0	−4.9	19 06 00 −03 00	60?	S?	22?	0.5?	3C396.1
32.1	−0.9	18 53 10 −01 08	40?	C?	?	?	
32.8	−0.1	18 51 25 −00 08	17	S?	11?	0.2?	Kes 78
33.2	−0.6	18 53 50 −00 02	18	S	3.5	varies	
33.6	+0.1	18 52 48 +00 41	10	S	22	0.5	Kes 79, 4C00.70, HC13
34.7	−0.4	18 56 00 +01 22	35 × 27	C	230	0.30	W44, 3C392
36.6	−0.7	19 00 35 +02 56	25?	S?	?	?	
36.6	+2.6	18 48 49 +04 26	17 × 13?	S	0.7?	0.5?	
39.2	−0.3	19 04 08 +05 28	8 × 6	C	18	0.6	3C396, HC24, NRAO 593
39.7	−2.0	19 12 20 +04 55	120 × 60	?	85?	0.7?	W50, SS433
40.5	−0.5	19 07 10 +06 31	22	S	11	0.5	
41.1	−0.3	19 07 34 +07 08	4.5 × 2.5	S	22	0.48	3C397
42.8	+0.6	19 07 20 +09 05	24	S	3?	0.5?	
43.3	−0.2	19 11 08 +09 06	4 × 3	S	38	0.48	W49B
43.9	+1.6	19 05 50 +10 30	60?	S?	8.6?	0.2?	
45.7	−0.4	19 16 25 +11 09	22	S	4.2?	0.4?	

Table A1. (continued).

l	b	RA (J2000) Dec (h m s) (° ′)	size /arcmin	type	Flux at 1 GHz/Jy	spectral index	other name(s)
46.8	−0.3	19 18 10 +12 09	17 × 13	S	14	0.5	(HC30)
49.2	−0.7	19 23 50 +14 06	30	S?	160?	0.3?	(W51)
53.6	−2.2	19 38 50 +17 14	33 × 28	S	8	0.75	3C400.2, NRAO 611
54.1	+0.3	19 30 31 +18 52	1.5	F?	0.5	0.1	
54.4	−0.3	19 33 20 +18 56	40	S	28	0.5	(HC40)
55.0	+0.3	19 32 00 +19 50	20 × 15?	S	0.5?	0.5?	
55.7	+3.4	19 21 20 +21 44	23	S	1.4	0.6	
57.2	+0.8	19 34 59 +21 57	12?	S?	1.8?	?	(4C21.53)
59.5	+0.1	19 42 33 +23 35	5	S	3?	?	
59.8	+1.2	19 38 55 +24 19	20 × 16?	?	1.6	0.5	
63.7	+1.1	19 47 52 +27 45	8	F	1.8	0.3	
65.1	+0.6	19 54 40 +28 35	90 × 50	S	6	0.6	
65.3	+5.7	19 33 00 +31 10	310 × 240	S?	52?	0.6?	
65.7	+1.2	19 52 10 +29 26	18	?	5.1	0.6	DA 495
67.7	+1.8	19 54 32 +31 29	9	S	1.4	0.3	
68.6	−1.2	20 08 40 +30 37	28 × 25?	?	0.7?	0.0?	
69.0	+2.7	19 53 20 +32 55	80?	?	120?	varies	CTB 80
69.7	+1.0	20 02 40 +32 43	16	S	1.6	0.8	
73.9	+0.9	20 14 15 +36 12	22?	S?	9?	0.3?	
74.0	−8.5	20 51 00 +30 40	230 × 160	S	210	varies	Cygnus Loop
74.9	+1.2	20 16 02 +37 12	8 × 6	F	9	varies	CTB 87
76.9	+1.0	20 22 20 +38 43	12 × 9	?	2	0.6	
78.2	+2.1	20 20 50 +40 26	60	S	340	0.5	DR4, γ Cygni SNR
82.2	+5.3	20 19 00 +45 30	95 × 65	S	120?	0.5?	W63
84.2	−0.8	20 53 20 +43 27	20 × 16	S	11	0.5	
84.9	+0.5	20 50 30 +44 53	6	S	0.8	0.4	
85.4	+0.7	20 50 40 +45 22	24	S	?	0.5?	
85.9	−0.6	20 58 40 +44 53	24	S	?	0.5?	
89.0	+4.7	20 45 00 +50 35	120 × 90	S	220	0.40	HB21
93.3	+6.9	20 52 25 +55 21	27 × 20	S	9	0.54	DA 530, 4C(T)55.38.1
93.7	−0.2	21 29 20 +50 50	80	S	65	0.4	CTB 104A, DA 551
94.0	+1.0	21 24 50 +51 53	30 × 25	S	15	0.44	3C434.1
106.3	+2.7	22 27 30 +60 50	60 × 24	?	6	0.6	
109.1	−1.0	23 01 35 +58 53	28	S	20	0.50	CTB 109
111.7	−2.1	23 23 26 +58 48	5	S	2720	0.77	Cassiopeia A, 3C461

Table A1. (continued).

l	*b*	RA (J2000) Dec (h m s) (° ′)	size /arcmin	type	Flux at 1 GHz/Jy	spectral index	other name(s)
114.3	+0.3	23 37 00 +61 55	90 × 55	S	6?	0.3?	
116.5	+1.1	23 53 40 +63 15	80 × 60	S	11?	0.8?	
116.9	+0.2	23 59 10 +62 26	34	S	9?	0.5?	CTB 1
119.5	+10.2	00 06 40 +72 45	90?	S	36	0.6	CTA 1
120.1	+1.4	00 25 18 +64 09	8	S	56	0.61	Tycho, 3C10, SN1572
126.2	+1.6	01 22 00 +64 15	70	S?	7	varies	
127.1	+0.5	01 28 20 +63 10	45	S	13	0.6	R5
130.7	+3.1	02 05 41 +64 49	9 × 5	F	33	0.10	3C58, SN1181
132.7	+1.3	02 17 40 +62 45	80	S	45	0.6	HB3
156.2	+5.7	04 58 40 +51 50	110	S	5	0.5	
160.9	+2.6	05 01 00 +46 40	140 × 120	S	110	0.6	HB9
166.0	+4.3	05 26 30 +42 56	55 × 35	S	7?	0.4?	VRO 42.05.01
166.2	+2.5	05 19 00 +41 55	90 × 70	S	11	0.5	OA 184
179.0	+2.6	05 53 40 +31 05	70	S?	7	0.4	
180.0	−1.7	05 39 00 +27 50	180	S	65	varies	S147
182.4	+4.3	06 08 10 +29 00	50	S	1.2	0.4	
184.6	−5.8	05 34 31 +22 01	7 × 5	F	1040	0.30	Crab Nebula, 3C144, SN1054
189.1	+3.0	06 17 00 +22 34	45	C	160	0.36	IC443, 3C157
192.8	−1.1	06 09 20 +17 20	78	S	20?	0.6?	PKS 0607+17
205.5	+0.5	06 39 00 +06 30	220	S	160	0.5	Monoceros Nebula
206.9	+2.3	06 48 40 +06 26	60 × 40	S?	6	0.5	PKS 0646+06
260.4	−3.4	08 22 10 −43 00	60 × 50	S	130	0.5	Puppis A, MSH 08−44
261.9	+5.5	09 04 20 −38 42	40 × 30	S	10?	0.4?	
263.9	−3.3	08 34 00 −45 50	255	C	1750	varies	Vela (XYZ)
266.2	−1.2	08 52 00 −46 20	120	S	50?	0.3?	
272.2	−3.2	09 06 50 −52 07	15?	S?	0.4	0.6	
279.0	+1.1	09 57 40 −53 15	95	S	30?	0.6?	
284.3	−1.8	10 18 15 −59 00	24?	S	11?	0.3?	MSH 10−5*3*
286.5	−1.2	10 35 40 −59 42	26 × 6	S?	1.4?	?	
289.7	−0.3	11 01 15 −60 18	18 × 14	S	6.2	0.2?	
290.1	−0.8	11 03 05 −60 56	19 × 14	S	42	0.4	MSH 11−6*1*A
291.0	−0.1	11 11 54 −60 38	15 × 13	C	16	0.29	(MSH 11−6*2*)
292.0	+1.8	11 24 36 −59 16	12 × 8	C	15	0.4	MSH 11−5*4*
292.2	−0.5	11 19 20 −61 28	20 × 15	S	7?	0.6?	
293.8	+0.6	11 35 00 −60 54	20	C	5?	0.6?	

Table A1. (continued).

l	b	RA (J2000) Dec (h m s) (° ′)	size /arcmin	type	Flux at 1 GHz/Jy	spectral index	other name(s)
294.1	−0.0	11 36 10 −61 38	40	S	>2?	?	
296.1	−0.5	11 51 10 −62 34	37 × 25	S	8?	0.6?	
296.5	+10.0	12 09 40 −52 25	90 × 65	S	48	0.5	PKS 1209−51/52
296.8	−0.3	11 58 30 −62 35	20 × 14	S	9	0.6	1156−62
298.5	−0.3	12 12 40 −62 52	5?	?	5?	0.4?	
298.6	−0.0	12 13 41 −62 37	12 × 9	S	5?	0.3	
299.2	−2.9	12 15 13 −65 30	18 × 11	S	0.5?	?	
299.6	−0.5	12 21 45 −63 09	13	S	1.0?	?	
301.4	−1.0	12 37 55 −63 49	37 × 23	S	2.1?	?	
302.3	+0.7	12 45 55 −62 08	17	S	5?	0.4?	
304.6	+0.1	13 05 59 −62 42	8	S	14	0.5	Kes 17
308.1	−0.7	13 37 37 −63 04	13	S	1.2?	?	
308.8	−0.1	13 42 30 −62 23	30 × 20?	C?	15?	0.4?	
309.2	−0.6	13 46 31 −62 54	15 × 12	S	7?	0.4?	
309.8	+0.0	13 50 30 −62 05	25 × 19	S	17	0.5	
310.6	−0.3	13 58 00 −62 09	8	S	5?	?	Kes 20B
310.8	−0.4	14 00 00 −62 17	12	S	6?	?	Kes 20A
311.5	−0.3	14 05 38 −61 58	5	S	3?	0.5	
312.4	−0.4	14 13 00 −61 44	38	S	45	0.36	
312.5	−3.0	14 21 00 −64 12	18 × 20	S	3.5?	?	
315.4	−2.3	14 43 00 −62 30	42	S	49	0.6	RCW 86, MSH 14−63
315.4	−0.3	14 35 55 −60 36	24 × 13	?	8	0.4	
315.9	−0.0	14 38 25 −60 11	25 × 14	S	0.8?	?	
316.3	−0.0	14 41 30 −60 00	29 × 14	S	20?	0.4	(MSH 14−57)
317.3	−0.2	14 49 40 −59 46	11	S	4.7?	?	
318.2	+0.1	14 54 50 −59 04	40 × 35	S	>3.9?	?	
318.9	+0.4	14 58 30 −58 29	30 × 14	C	4?	0.2?	
320.4	−1.2	15 14 30 −59 08	35	C	60?	0.4	MSH 15−52, RCW 89
320.6	−1.6	15 17 50 −59 16	60 × 30	S	?	?	
321.9	−1.1	15 23 45 −58 13	28	S	>3.4?	?	
321.9	−0.3	15 20 40 −57 34	31 × 23	S	13	0.3	
322.5	−0.1	15 23 23 −57 06	15	C	1.5	0.4	
323.5	+0.1	15 28 42 −56 21	13	S	3?	0.4?	
326.3	−1.8	15 53 00 −56 10	38	C	145	varies	MSH 15−56
327.1	−1.1	15 54 25 −55 09	18	C	7?	?	

Table A1. (continued).

l	b	RA (J2000) Dec (h m s) (° ′)	size /arcmin	type	Flux at 1 GHz/Jy	spectral index	other name(s)
327.4	+0.4	15 48 20 −53 49	21	S	30?	0.6	Kes 27
327.4	+1.0	15 46 48 −53 20	14	S	1.9?	?	
327.6	+14.6	15 02 50 −41 56	30	S	19	0.6	SN1006, PKS 1459−41
328.4	+0.2	15 55 30 −53 17	5	F	15	0.12	(MSH 15−57)
329.7	+0.4	16 01 20 −52 18	40 × 33	S	>34?	?	
330.0	+15.0	15 10 00 −40 00	180?	S	350?	0.5?	Lupus Loop
330.2	+1.0	16 01 06 −51 34	11	S?	5?	0.3	
332.0	+0.2	16 13 17 −50 53	12	S	8?	0.5	
332.4	−0.4	16 17 33 −51 02	10	S	28	0.5	RCW 103
332.4	+0.1	16 15 20 −50 42	15	S	26	0.5	MSH 16−5*1*, Kes 32
335.2	+0.1	16 27 45 −48 47	21	S	16	0.5	
336.7	+0.5	16 32 11 −47 19	14 × 10	S	6	0.5	
337.0	−0.1	16 35 57 −47 36	1.5	S	1.5	0.6?	(CTB 33)
337.2	−0.7	16 39 28 −47 51	6	S	2?	0.7	
337.3	+1.0	16 32 39 −46 36	15 × 12	S	16	0.55	Kes 40
337.8	−0.1	16 39 01 −46 59	9 × 6	S	18	0.5	Kes 41
338.1	+0.4	16 37 59 −46 24	15?	S	4?	0.4	
338.3	−0.0	16 41 00 −46 34	8	S	7?	?	
338.5	+0.1	16 41 09 −46 19	9	?	12?	?	
340.4	+0.4	16 46 31 −44 39	10 × 7	S	5	0.4	
340.6	+0.3	16 47 41 −44 34	6	S	5?	0.4?	
341.2	+0.9	16 47 35 −43 47	16 × 22	C	1.5?	0.6?	
341.9	−0.3	16 55 01 −44 01	7	S	2.5	0.5	
342.0	−0.2	16 54 50 −43 53	12 × 9	S	3.5?	0.4?	
342.1	+0.9	16 50 43 −43 04	10 × 9	S	0.5?	?	
343.0	−6.0	17 25 00 −46 30	250	S	?	?	
343.1	−2.3	17 08 00 −44 16	32?	C?	8?	0.5?	
343.1	−0.7	17 00 25 −43 14	27 × 21	S	7.8	0.55	
344.7	−0.1	17 03 51 −41 42	10	C?	2.5?	0.5	
345.7	−0.2	17 07 20 −40 53	6	S	0.6?	?	
346.6	−0.2	17 10 19 −40 11	8	S	8?	0.5?	
347.3	−0.5	17 13 50 −39 45	65 × 55	S?	?	?	
348.5	−0.0	17 15 26 −38 28	10?	S?	10?	0.4?	
348.5	+0.1	17 14 06 −38 32	15	S	72	0.3	CTB 37A
348.7	+0.3	17 13 55 −38 11	17?	S	26	0.3	CTB 37B

Table A1. (continued).

l	b	RA (J2000) Dec (h m s) (° ′)	size /arcmin	type	Flux at 1 GHz/Jy	spectral index	other name(s)
349.2	−0.1	17 17 15 −38 04	9 × 6	S	1.4?	?	
349.7	+0.2	17 17 59 −37 26	2.5 × 2	S	20	0.5	
350.0	−2.0	17 27 50 −38 32	45	S	26	0.4	
351.2	+0.1	17 22 27 −36 11	7	C?	5?	0.4	
351.7	+0.8	17 21 00 −35 27	18 × 14	S	10?	?	
351.9	−0.9	17 28 52 −36 16	12 × 9	S	1.8?	?	
352.7	−0.1	17 27 40 −35 07	8 × 6	S	4	0.6	
353.9	−2.0	17 38 55 −35 11	13	S	1?	0.5?	
354.1	+0.1	17 30 28 −33 46	15 × 3?	C?	?	varies?	
354.8	−0.8	17 36 00 −33 42	19	S	2.8?	?	
355.6	−0.0	17 35 16 −32 38	8 × 6	S	3?	?	
355.9	−2.5	17 45 53 −33 43	13	S	8	0.5	
356.2	+4.5	17 19 00 −29 40	25	S	4	0.7	
356.3	−0.3	17 37 56 −32 16	11 × 7	S	3?	?	
356.3	−1.5	17 42 35 −32 52	20 × 15	S	3?	?	
357.7	−0.1	17 40 29 −30 58	8 × 3?	?	37	0.4	MSH 17−3*9*
357.7	+0.3	17 38 35 −30 44	24	S	10	0.4?	
358.0	+3.8	17 26 00 −28 36	38	S	1.5?	?	
359.0	−0.9	17 46 50 −30 16	23	S	23	0.5	
359.1	−0.5	17 45 30 −29 57	24	S	14	0.4?	
359.1	+0.9	17 39 36 −29 11	12 × 11	S	5?	?	